Solution of nonlinear vibration problem of shear deformable multilayer nonhomogeneous orthotropic plates using Poincare-Lindstedt method

SOLUTION OF NONLINEAR VIBRATION PROBLEM OF SHEAR DEFORMABLE MULTILAYER NONHOMOGENEOUS ORTHOTROPIC PLATES USING POINCARE-LINDSTEDT METHOD

[a,b,c]AVEY M., [d]FANTUZZI N., [e*,f,h]SOFIYEV A.H.

[a]Department of Mathematical Engineering, Graduate School of Istanbul TechnicalUniversity, 34469 Maslak/Istanbul, Turkey; avey22@itu.edu.tr ORCID: 0000-0002-9963 0955
[b]Analytical Information Resources Center of UNEC-Azerbaijan State Economics University, 1001/Baku, Azerbaijan
[c]Application and Research Center, Istanbul Ticaret University, 34445 Istanbul, Turkey
[d]Department of Civil, Chemical, Environmental, and Materials Engineering, UniversityBologna, 40136 Bologna, Italy; nicholas.fantuzzi@unibo.it
[e*]Department of Mathematics, Istanbul Ticaret University, Beyoglu 34445/Istanbul, Turkey ORCID: 0000-0001-7678-6351
[f]Scientific Research Department of Azerbaijan University of Architecture and Construction, Baku 1073, Azerbaijan
[h]Scientific Research Centers for Composition Materials of UNEC Azerbaijan State Economic University, Baku 100 Azerbaijan

TOTAL NUMBER OF PAGES: 36, FIGURES: 8, TABLES: 6

Corresponding author: **Prof. Dr. ABDULLAH H. SOFIYEV**
Department of Mathematics, Istanbul Ticaret University,
Beyoglu 34445/Istanbul, Turkey
Tel: +90 444 0 413 4142
Fax: 00 90 246 237 0859

ABSTRACT

In this study, one of the first attempts is made to solve the nonlinear (NL) vibration problem of shear-deformable multilayer plates consisting of nonhomogeneous orthotropic layers (NHOLs) using the Poincaré-Lindstedt method. First, the shear deformation theory (SDT) for homogeneous plates is extended to multilayer plates composed of NHOLs. In the framework of von-Karman type nonlinear theory, the basic relations of the plates in question are established and then NL equations of motion based on four functions such as rotation angles, Airy stress and deflection functions are derived. Then, NL-partial differential equations (NL-PDEs) are reduced to NL-ordinary differential equations (NL-ODE) and the solution of NL-ODE is performed for the first time by the modified Poincaré -Lindstedt method, yielding new amplitude dependent expressions for NL frequency, and for the ratio of NL frequency to linear (NL/L) frequency for multilayer plates consisting of NHOLs. Finally, detailed parametric studies are carried out to gain insight into the effects of various factors such as shear strains, non-homogeneity, number and array of layers on the NL frequencies under different rectangular plate characteristics.

Keywords: Non-homogeneity, multilayer plates, nonlinear vibration, Poincaré -Lindstedt method

1. Introduction

The desire to lighten the structure without reducing its carrying capacity has led to the use of plate-shaped structural elements. The plates with various configurations are widely used in engineering structures, mechanical engineering, shipbuilding, aerospace industry and rocket technology. In connection with the increase in the power and movement speed of the mechanisms, it is becoming increasingly important to examine the dynamic behavior, especially the vibration behavior, of the plates used as their components. The reliability of the dynamic behavior of structural elements requires realistic modeling of their mechanical properties. Structural elements created from composite materials have a pronounced anisotropy of deformation properties, low resistance to transverse deformations and a number of such features. Realistic analyzes require the use of improved theories, since the use of classical shell theory, which neglects these factors, in some cases leads to significant errors in numerical calculations. The natural evolution of plate theory, widely presented in the literature, has led, in particular, to the formation and development of multilayer plate theories [1, 2]. The first studies on multilayer anisotropic plates and detailed information on their development history are presented in the monographs [3-5]. In these studies, the main formulations of boundary value problems in multilayer anisotropic plate theory were formulated, methods for solving them were developed and practical applications were realized. It is very important to examine the dynamic problems of multilayer structural elements within the framework of nonlinear models, taking into account the realistic physical and mechanical properties of the materials forming each layer. As mentioned above, significant research has been conducted on the nonlinear vibrations of multilayer plates consisting of homogeneous orthotropic layers, most of them using finite element methods [6-15].

In contrast to the study of various dynamic behavior of multilayer homogeneous structural elements, solving dynamic problems of non-homogeneous multilayer structural elements is

associated with significant difficulties. These difficulties arise both because of the complexity of modern structures, which include structural elements with different properties and heterogeneity, and because of the extreme operating conditions of promising composite materials with pronounced anisotropy being introduced to the market and high requirements for their reliability. Among the various reasons that create heterogeneity in materials, the most common are humidity, radiation, excessive temperature, thermal polishing, etc. In some operating conditions, very strong thermal effects can also disrupt the homogeneity of the material in a certain part of the structural elements. As a result of various influences, the mechanical properties of homogeneous orthotropic materials can be transformed into continuous, piecewise continuous and random functions of point coordinates. This makes it necessary, when setting problems related to vibrations of multilayer structural elements, to take into account the heterogeneity and orthotropy of materials in the layers and study their influence on the nonlinear frequency-amplitude dependence. As is known, although efforts to create analytical models that reflect the reality of the mechanical properties of non-homogeneous anisotropic materials are always on the agenda, the number of modeling studies is limited [16-21].

One of the main goals when designing multilayer structural elements is to make their vibration calculations. In most cases, in the linear and nonlinear vibration calculations of structural elements consisting of homogeneous materials, it is seen that their frequencies are much different than in reality. One of the reasons for this phenomenon lies in the heterogeneous anisotropic nature of the layers forming the layered structural element. To date, many studies have been carried out on linear and nonlinear vibrations of multilayer homogeneous orthotropic plates. The majority of these studies focused on the solution of linear vibration problems [22-36], and relatively few studies were carried out in non-linear formulation [37-42].

Calculating the vibration analysis of homogeneous and non-homogeneous structural systems with any of the numerical methods does not pose a serious fundamental difficulty. However, analytical results provide a qualitative understanding of the subject and help in correctly formulating problems in numerical simulation and checking the results. There are different analytical methods for solving nonlinear ordinary differential equations. Perturbation techniques are a class of analytical methods used to determine approximate solutions to nonlinear differential equations for which exact solutions cannot be obtained. They are useful to illustrate, predict and explain phenomena caused by nonlinear effects in the vibration of structural members. They can also be applied to nonlinear and linear systems with variable coefficients and/or complex boundary conditions where exact solutions in closed form are not known. In this study, the nonlinear behavior of plates with inhomogeneous orthotropic layers will be solved by the Poincaré-Lindstedt method. The Poincaré-Lindstedt method is an extension of the straightforward perturbation method to eliminate secular terms and find the periodic solution of NL-ODEs. The perturbation series solution will be similar to the straightforward method. To eliminate secular terms, the vibration frequency perturbation parameter is replaced by another polynomial series. The coefficients of this polynomial are determined by eliminating secular terms. To apply the Poincaré-Lindstedt method, the NL-ODEs must have a periodic response potential. Studies reveal that the nonlinear vibration problem of multilayer plates with non-homogeneous orthotropic layers based on SDT cannot be solved by the Poincaré-Lindstedt method. This study is aimed at solving the problem by applying the method in question.

2. Formulation of the problem

Consider a moderately-thick multilayer plate with total thickness h, lengths a and b on the x and y axes, respectively, which consists of heterogeneous orthotropic N layers. The

geometry, coordinate system and the cross-section o multilayer plates are shown in Fig. 1. The origin of the coordinate system $Oxyz$ is in the upper left corner of the reference plane of the multilayer plate, while the x and y axes are on the $z=0$ reference plane, the z axis is perpendicular to the reference plane and directed inwards. The $z=0$ reference plane is located at the interface of the layers at even values of N, while at odd values of N the reference plane is located at the reference plane of the middle layer.

It is assumed that the layers of multilayer plate are perfectly bonded to each other, they do not slip and remain elastic during deformation. Let's assume that the main elasticity axes of each layer are parallel to the coordinate axes on the reference plane. The displacements in the x, y and z directions are indicated by U,V and W, $\varphi_1(x,y,t)$ and $\varphi_2(x,y,t)$ are rotations of the normals to the middle plane relative to the y and x axes, respectively. Let $\Psi(x,y,t)$ be the Airy stress function for the stress resultants, so that [3-5],

$$N_{11}=h\frac{\partial^2\Psi}{\partial y^2},\ N_{22}=h\frac{\partial^2\Psi}{\partial x^2},\ \ N_{12}=-h\frac{\partial^2\Psi}{\partial x\partial y} \tag{1}$$

The mechanical properties of lamina k^{th} are power law function of the thickness coordinate and defined as follows [17-20]:

$$\begin{gathered}E_{11Z}^{(k)}=\left[1+\eta_1 Z^{\chi}\right]E_{11}^{0(k)},\ E_{22Z}^{(k)}=\left[1+\eta_1 Z^{\chi}\right]E_{22}^{0(k)},\ G_{12Z}^{(k)}=\left[1+\eta_1 Z^{\chi}\right]G_{12}^{0(k)},\\ G_{13Z}^{(k)}=\left[1+\eta_1 Z^{\chi}\right]G_{13}^{0(k)},\ G_{23Z}^{(k)}=\left[1+\eta_1 Z^{\chi}\right]G_{23}^{0(k)},\ \rho_Z^{(k)}=\left[1+\eta_2 Z^{\chi}\right]\rho^{0(k)},\ Z=z/h\end{gathered} \tag{2}$$

where $E_{ii}^{(k)}$, $G_{ij}^{(k)}(i=1,2,j=2,3)$ and $\rho_Z^{(k)}$ are Young moduli, shear moduli and density of heterogeneous orthotropic materials in the lamina k^{th}, χ is the is the power exponent and is a positive integer, the symbols with "0" in the superscript indicate the mechanical properties of the homogeneous orthotropic material, η_1 and η_2 indicate the non-homogeneity parameter for the elasticity moduli and density, respectively, in the k^{th} layer of multilayer plates, which characterizes its variation depending on the Z and $\eta_i \in [-1,1]$. In addition, $\nu_{12}^{(k)}$ and $\nu_{21}^{(k)}$ are Poisson ratios are considered constant since the effect of heterogeneity according to the thickness coordinate is very small and the following condition is satisfied: $\nu_{21}^{(k)} E_{11}^{0(k)} = \nu_{12}^{(k)} E_{22}^{0(k)}$ and $\eta_i = 0$ indicates homogeneous orthotropic material.

3. Basic equations

Based on the Ambartsumyan's shear deformation theory with the von Kármán-type of kinematic non-linearity the motion equations for the shear deformable multilayer plates could be expressed as [3]:

$$\begin{aligned}
&\frac{\partial M_{11}}{\partial x}+\frac{\partial M_{12}}{\partial y}-Q_1+\rho_1\frac{\partial^3 W}{\partial x\partial t^2}-\rho_2\frac{\partial^2 \varphi_1}{\partial t^2}=0\\
&\frac{\partial M_{21}}{\partial x}+\frac{\partial M_{22}}{\partial y}-Q_2+\rho_1\frac{\partial^3 W}{\partial y\partial t^2}-\rho_3\frac{\partial^2 \varphi_2}{\partial t^2}=0\\
&\frac{\partial Q_1}{\partial x}+\frac{\partial Q_2}{\partial y}+N_{11}\frac{\partial^2 W}{\partial x^2}+2N_{12}\frac{\partial^2 W}{\partial x\partial y}+N_{22}\frac{\partial^2 W}{\partial y^2}=\overline{\rho}\frac{\partial^2 W}{\partial t^2}
\end{aligned} \tag{3}$$

The strain compatibility equation can be given as follows:

$$\frac{\partial^2 e_{11}^0}{\partial y^2}+\frac{\partial^2 e_{22}^0}{\partial x^2}-\frac{\partial^2 \gamma_{12}^0}{\partial x\partial y}=\left(\frac{\partial^2 W}{\partial x\partial y}\right)^2-\frac{\partial^2 W}{\partial x^2}\frac{\partial^2 W}{\partial y^2} \tag{4}$$

where e_{ii}^0 and γ_{12}^0 are strains in the reference plane and t is a time. Here in-plane forces (N_{ij}), shear forces $\left(Q_j\right)$ and moments $\left(M_{ij}\right)$, the normal and rotary inertia coefficients $\overline{\rho}$ and $\rho_i(i=1,2,3)$ are defined, respectively, as follows:

$$\left(N_{ij},\, Q_j\right)=\sum_{k=1}^{N}\int_{z_{k-1}}^{z_k}\left(\sigma_{ij}^{(k)},\sigma_{1j_1}^{(k)}\right)\mathrm{d}z, M_{ij}=\sum_{k=1}^{N}\int_{z_{k-1}}^{z_k}\sigma_{ij}^{(k)}z\mathrm{d}z,\ (i,j=1,2,j_1=2,3) \tag{5}$$

$$\overline{\rho}=\sum_{k=1}^{N}\int_{z_{k-1}}^{z_k}\rho_t^{(k)}\mathrm{d}z,\ \rho_1=\sum_{k=1}^{N}\int_{z_{k-1}}^{z_k}\rho^{(k)}z^2\mathrm{d}z,\ \ \rho_2=\sum_{k=1}^{N}\int_{z_{k-1}}^{z_k}\Delta_{1z}^{(k)}\rho^{(k)}z\mathrm{d}z,\ \ \rho_3=\sum_{k=1}^{N}\int_{z_{k-1}}^{z_k}\Delta_{2z}^{(k)}\rho^{(k)}z\mathrm{d}z. \tag{6}$$

in which $-\frac{h}{2}+\frac{(k-1)h}{N}\le z\le -\frac{h}{2}+\frac{kh}{N}$ and $\Delta_{jz}^{(k)}(j=1,2)$ are the parameters containing the shear stress shape function and is defined in the next stage.

The relationships between stresses $\sigma_{ij}^{(k)}(i=1,2,j=1,2,3)$, and strains e_{ii} and γ_{ij} for the k^{th} lamina contained in multilayer plates composed of NHOLs can be written as follows [17-19, 27],

$$\begin{pmatrix}\sigma_{11}^{(k)}\\ \sigma_{22}^{(k)}\\ \sigma_{12}^{(k)}\\ \sigma_{13}^{(k)}\\ \sigma_{23}^{(k)}\end{pmatrix}=\begin{bmatrix}\overline{E}_{11Z}^{(k)} & \overline{E}_{12Z}^{(k)} & 0 & 0 & 0\\ \overline{E}_{21Z}^{(k)} & \overline{E}_{22Z}^{(k)} & 0 & 0 & 0\\ 0 & 0 & \overline{E}_{66Z}^{(k)} & 0 & 0\\ 0 & 0 & 0 & \overline{E}_{55Z}^{(k)} & 0\\ 0 & 0 & 0 & 0 & \overline{E}_{44Z}^{(k)}\end{bmatrix}\begin{bmatrix}e_{11}\\ e_{22}\\ \gamma_{12}\\ \gamma_{13}\\ \gamma_{23}\end{bmatrix} \tag{7}$$

where

$$\begin{aligned}
&\overline{E}_{11Z}^{(k)} = \frac{E_{11Z}^{(k)}}{1-\nu_{12}^{(k)}\nu_{21}^{(k)}},\ \overline{E}_{12Z}^{(k)} = \frac{\nu_{21}^{(k)}E_{11Z}^{(k)}}{1-\nu_{12}^{(k)}\nu_{21}^{(k)}} = \frac{\nu_{12}^{(k)}E_{22Z}^{(k)}}{1-\nu_{12}^{(k)}\nu_{21}^{(k)}} = \overline{E}_{21Z}^{(k)} \\
&\overline{E}_{22Z}^{(k)} = \frac{E_{22Z}^{(k)}}{1-\nu_{12}^{(k)}\nu_{21}^{(k)}}, \overline{E}_{44Z}^{(k)} = G_{23Z}^{(k)},\ \overline{E}_{55Z}^{(k)} = G_{13Z}^{(k)},\ \overline{E}_{66Z}^{(k)} = G_{12Z}^{(k)}
\end{aligned} \tag{8}$$

in which $E_{ii}^{(k)},\ G_{ij}^{(k)}(i,j=1,2,3)$ are Young and shear moduli of heterogeneous orthotropic materials in the lamina k^{th}, $\nu_{12}^{(k)}$ and $\nu_{21}^{(k)}$ are Poisson ratios and are considered constant since the effect of nonhomogeneity according to the thickness coordinate is very small and the following condition is satisfied: $\nu_{21}^{(k)}E_{11}^{0(k)} = \nu_{12}^{(k)}E_{22}^{0(k)}$.

Considering the assumptions of the SDT proposed by Ambartsumian [3] and extending this theory to non-homogeneous multilayer orthotropic plates, the shear stresses $\sigma_{13}^{(k)}$ and $\sigma_{23}^{(k)}$ in the lamina k^{th} are defined as follows [3, 34]:

$$\sigma_{13}^{(k)} = \frac{df_1^{(k)}}{dz}\varphi_1(x,y,t),\ \sigma_{23}^{(k)} = \frac{df_2^{(k)}}{dz}\varphi_2(x,y,t) \tag{9}$$

where $\frac{df_i^{(k)}}{dz}\ (i=1,2)$ are shear stress functions.

When the theory of nonlinear shells is applied within the framework of shear deformation theory and using the relationship (9), correlations between the unit strains of any point not located in the mid-plane of the multilayer plates composed of NHOLs and the strains, curvatures and transverse shear strains on the mid-plane can be established as follows [34]:

$$\begin{bmatrix} e_{11} \\ e_{22} \\ \gamma_{12} \end{bmatrix} = \begin{bmatrix} e_{11}^0 - z\dfrac{\partial^2 W}{\partial x^2} + \Delta_{1z}^{(k)}\dfrac{\partial \varphi_1}{\partial x} \\ e_{22}^0 - z\dfrac{\partial^2 W}{\partial y^2} + \Delta_{2z}^{(k)}\dfrac{\partial \varphi_2}{\partial y} \\ \gamma_{12}^0 - 2z\dfrac{\partial^2 W}{\partial x \partial y} + \Delta_{1z}^{(k)}\dfrac{\partial \varphi_1}{\partial y} + \Delta_{2z}^{(k)}\dfrac{\partial \varphi_2}{\partial x} \end{bmatrix} \tag{10}$$

where

$$\begin{bmatrix} e_{11}^0 \\ e_{22}^0 \\ \gamma_{12}^0 \end{bmatrix} = \begin{bmatrix} \dfrac{\partial U}{\partial x} + \dfrac{1}{2}\left(\dfrac{\partial W}{\partial x}\right)^2 \\ \dfrac{\partial V}{\partial y} + \dfrac{1}{2}\left(\dfrac{\partial W}{\partial y}\right)^2 \\ \dfrac{\partial V}{\partial x} + \dfrac{\partial U}{\partial y} + \dfrac{\partial W}{\partial x}\dfrac{\partial U}{\partial \mathrm{y}} \end{bmatrix} \tag{11}$$

in which

$$\Delta_{1z}^{(k)} = \int_0^z \frac{1}{G_{13z}^{(\mathrm{k})}} \frac{\mathrm{d}f_1^{(\mathrm{k})}}{\mathrm{d}z}\mathrm{d}z, \Delta_{2z}^{(k)} = \int_0^z \frac{1}{G_{23z}^{(\mathrm{k})}} \frac{\mathrm{d}f_2^{(k)}}{\mathrm{d}z}\mathrm{d}z \tag{12}$$

The expressions obtained by substituting relations (10) in the Eq. (7) are substituted in Eqs. (1) and (5) and after mathematical operations, unit strains at the middle surface, moments and shear forces are expressed with independent parameters $\Psi, W, \varphi_1, \varphi_2$. Then, these relations are substituted into the system of equations (3) and (4), the nonlinear motion and deformation compatibility equations for multilayer plates composed of NHOLs within SDT are obtained as follows:

$$L_{11}(\Psi)+L_{12}(W)+L_{13}(\varphi_1)+L_{14}(\varphi_1)=0$$

$$L_{21}(\Psi)+L_{22}(W)+L_{23}(\varphi_1)+L_{24}(\varphi_2)=0 \tag{13}$$

$$L_{31}(\Psi)+L_{32}(W)+L_{33}(\varphi_1)+L_{34}(\varphi_2)+L_{35}(\Psi,W)=0$$

and

$$L_{41}(\Psi)+L_{42}(W)+L_{43}(\varphi_1)+L_{44}(\varphi_2)+L_{45}(W,W)=0 \tag{14}$$

where $L_{ij}(i=1,2,...,4,\ j=1,2,..,5)$ are the nonlinear differential operators (refer Appendix: A).

4. Solution procedure

Since all edges of multilayer plates are assumed to be simply supported, the system of equations (13) and (14) is solved under the following boundary conditions [3, 4]:

$$\begin{aligned} &W=0,\ \ \varphi_2=0,\ \ \text{when } x=0,\ a \\ &W=0,\ \ \varphi_1=0,\ \ \text{when } y=0,\ b \end{aligned} \tag{15}$$

The solution of the geometric NL-PDE (14) providing simple-supported boundary conditions is sought as follows:

$$W=W_1(t)\sin(\eta_1 x)\sin(\eta_2 y),\ \varphi_1=\varphi_{11}(t)\cos(\eta_1 x)\sin(\eta_2 y),\ \varphi_2=\varphi_{22}(t)\sin(\eta_1 x)\cos(\eta_2 y) \tag{16}$$

where $W_1(t)$, $\varphi_{11}(t)$ and $\varphi_{22}(t)$ are time dependent functions, $\eta_1 = \frac{m\pi}{a}$ and $\eta_2 = \frac{n\pi}{b}$ are the wave parameters in which m, n) is the vibration mode.

Substituting the approximation functions (16) into the Eq. (14) and performing some mathematical operations, Airy stress function is expressed as follows:

$$\Psi = J_1(t)\cos(2\eta_1 x) + J_2(t)\cos(2\eta_2 y) + J_3(t)\sin(\eta_1 x)\sin(\eta_2 y) \tag{17}$$

where:

$$J_1(t) = \frac{q_{14}W_1^2(t)}{32m_1^4 q_3},\ J_2(t) = \frac{q_{14}W_1^2(t)}{32n_1^4 q_1},\ \ J_3(t) = \frac{q_{11}W_1(\mathrm{t}) + q_{12}\varphi_{11}(\mathrm{t}) + q_{13}\varphi_{22}(\mathrm{t})}{q_1 n_1^4 + q_2 m_1^2 n_1^2 + q_3 m_1^4} \tag{18}$$

in which

$$\begin{gathered} q_1 = r_{11}h,\ q_2 = (r_{12} + r_{21} + r_{31})h,\ q_3 = r_{22}h,\ q_{11} = r_{23}m_1^4 + (r_{24} + r_{13} - r_{32})m_1^2 n_1^2 + r_{14}n_1^4, \\ q_{12} = -\left[r_{25}m_1^3 - (r_{15} + r_{35})m_1 n_1^2\right],\ q_{13} = -\left[(r_{28} + r_{38})m_1^2 + r_{18}n_1^2\right]n_1,\ q_{14} = m_1^2 n_1^2 \end{gathered} \tag{19}$$

When the Galerkin method is applied by substituting the approximation functions defined by (16) and (17) into the system of Eqs. (13), the inertial forces created by the rotation angles are ignored due to their ineffectiveness, we obtain:

$$\begin{gathered} u_{11}W_1 + u_{11}^{NL}W_1^2 + u_{12}\varphi_{11} + u_{13}\varphi_{22} = 0 \\ u_{21}W_1 + u_{21}^{NL}W_1^2 + u_{22}\varphi_{11} + u_{23}\varphi_{22} = 0 \\ \bar{\rho}\frac{d^2W_1}{dt^2} + u_{31}W_1 + u_{31}^{NL}W_1^2 + u_{32}W_1^3 + u_{33}\varphi_{11} + u_{34}\varphi_{22} = 0 \end{gathered} \tag{20}$$

where $u_{ij}(i=1,2,3,\ j=1,2,3,4)$ are parameters depending on the characteristics of multilayer plates composed of NHOLs (refer Appendix: B).

The unknowns $\varphi_{11}(\mathrm{t})$ and $\varphi_{22}(\mathrm{t})$ are eliminated from the set of Eqs. (20), it turns into the following nonlinear ordinary differential equation depending on the time:

$$\bar{\rho}\frac{\mathrm{d}^2 W_1}{\mathrm{d}t^2}+\bar{u}_{31}W_1+\bar{u}_{31}^{NL}W_1^2+u_{32}W_1^3=0 \tag{21}$$

where

$$\begin{aligned}
&\bar{u}_{31}=u_{31}+\frac{u_{11}u_{23}u_{33}-u_{21}u_{13}u_{33}}{u_{22}u_{13}-u_{12}u_{23}}-u_{34}\left(\frac{u_{21}}{u_{23}}+\frac{u_{22}}{u_{23}}\frac{u_{11}u_{23}-u_{21}u_{13}}{u_{22}u_{13}-u_{23}u_{12}}\right),\\
&\bar{u}_{31}^{NL}=\frac{u_{31}^{NL}u_{23}-u_{34}u_{21}^{NL}}{u_{23}}-\frac{u_{11}^{NL}u_{23}u_{33}-u_{13}u_{21}^{NL}u_{33}}{u_{12}u_{23}-u_{13}u_{22}}+\frac{u_{34}u_{22}}{u_{23}}\frac{u_{11}^{NL}u_{23}-u_{13}u_{21}^{NL}}{u_{12}u_{23}-u_{13}u_{22}}
\end{aligned} \tag{22}$$

By using $\tau=\omega t,\ \bar{W}=W_1/h$, from the Eq.(21), one gets:

$$\frac{\mathrm{d}^2\bar{W}}{\mathrm{d}\tau^2}+\alpha\bar{W}+\beta\bar{W}^2+\gamma\bar{W}^3=0 \tag{23}$$

where

$$\alpha=\frac{\bar{u}_{31}}{\bar{\rho}\omega^2},\ \beta=\frac{\bar{u}_{31}^{NL}h}{\bar{\rho}\omega^2},\ \gamma=\frac{u_{32}h^2}{\bar{\rho}\omega^2} \tag{24}$$

The linear frequency (LF) of multilayer plates composed of NHOLs within SDT is defined as:

$$\omega_L^{ST} = \sqrt{\frac{\overline{u}_{31}}{\overline{\rho}}} \tag{25}$$

In order to apply the Poincaré-Lindstedt method to the solution of Eq. (23), a small parameter ε is introduced and it has been rewritten as follows [44]:

$$\frac{\mathrm{d}^2\overline{W}}{\mathrm{d}\tau^2} + \alpha\overline{W} + \varepsilon\overline{\beta}\overline{W}^2 + \varepsilon\overline{\gamma}\overline{W}^3 = 0 \tag{26}$$

where the following definitions apply: $\overline{\beta} = \frac{\beta}{\varepsilon}$, $\overline{\gamma} = \frac{\gamma}{\varepsilon}$.

The nonlinear ordinary differential Eq. (26) will be solved for the following initial conditions:

$$\overline{W} = A, \frac{\mathrm{d}\overline{W}}{d\tau} = 0 \ at \ \tau = 0 \tag{27}$$

where $A = \frac{W_{\max}}{h}$ is the dimensionless maximum vibration amplitude

When the Poincaré-Lindstedt method is applied to the Eq. (26), the expansion of $\overline{W}$ and α functions into power series are written as follows:

$$\overline{W} = \overline{W}_0 + \varepsilon\overline{W}_1 + \varepsilon^2\overline{W}_2 + ... \tag{28}$$

$$\alpha = \Omega^2 + \varepsilon p_1 + \varepsilon^2 p_2 + \ldots \tag{29}$$

where p_i and Ω denote the unknown parameters.

Substituting Eq. (28) and (29) into Eq. (26), and then collecting the coefficients of like powers of $\varepsilon^i (i = 0,1,2)$ gives a sequence of linear second –order differential equation system, the first three of which are:

$$\varepsilon^0 : \frac{\mathrm{d}^2 \bar{W}_0}{\mathrm{d}\tau^2} + \Omega^2 \bar{W}_0 = 0 \tag{30}$$

$$\varepsilon^1 : \frac{\mathrm{d}^2 \bar{W}_1}{\mathrm{d}\tau^2} + \Omega^2 \bar{W}_1 = -p_1 \bar{W}_0 - \bar{\beta} \bar{W}_0^2 - \bar{\gamma} \bar{W}_0^3 \tag{31}$$

$$\varepsilon^2 : \frac{\mathrm{d}^2 \bar{W}_2}{\mathrm{d}\tau^2} + \Omega^2 \bar{W}_2 = -p_2 \bar{W}_0 - p_1 \bar{W}_1 - 2\bar{\beta} \bar{W}_0 \bar{W}_1 - 3\bar{\gamma} \bar{W}_1 \bar{W}_0^2 \tag{32}$$

The solution of the homogeneous ODE (30) with the initial conditions $\bar{W}_0 = A$, $\frac{d\bar{W}_0}{d\tau} = 0$, is as follows:

$$\bar{W}_0 = A\cos(\Omega\tau) \tag{33}$$

When the expression (33) is substituted into Eq. (31), it turns into the following form:

$$\ddot{\bar{W}}_1 + \Omega^2 \bar{W}_1 = -\left(p_1 + \frac{3}{4}\bar{\gamma} A^2 \right) A\cos(\Omega\tau) - \frac{1}{2}\bar{\beta} A^2 \left[\cos(2\Omega\tau) - 1 \right] \tag{34}$$

By setting the secular term equal to zero in Eq. (34), we obtain:

$$p_1 = -\frac{3}{4}\gamma A^2 \tag{35}$$

Considering (35), the solution of the non-homogeneous ODE (34) with initial conditions

$\bar{W}_1 = \frac{d\bar{W}_1}{d\tau} = 0$, one gets:

$$\bar{W}_1 = \frac{A^2}{\Omega^2}\left[\left(\frac{\bar{\beta}}{3} - \frac{\bar{\gamma}A}{32}\right)\cos(\Omega\tau) + \frac{\bar{\beta}\left[\cos(2\Omega\tau) - 3\right]}{6} + \frac{\bar{\gamma}A}{32}\cos(3\Omega\tau)\right] \tag{36}$$

To find the p_2 coefficient, expressions (33) and (36) are substituted into Eq. (32) and the secular term is removed from the resulting equation:

$$p_2 = \frac{A^2}{2\Omega^2}\left(\frac{5\bar{\beta}^2}{3} - \bar{\beta}\bar{\gamma}A + \frac{3\bar{\gamma}^2A^2}{64}\right) \tag{37}$$

It is noted that Eq. (32) is satisfied the following initial conditions: $\bar{W}_2 = \frac{d\bar{W}_2}{d\tau} = 0$.

When p_1 and p_2 are substituted into Eq. (29), the following fourth order algebraic equation is obtained as a result of simple mathematical operations:

$$\Omega^4-\left[\left(\omega_L^{ST}\right)^2+\frac{3}{4}\gamma A^2\right]\Omega^2+\frac{5\beta^2A^2}{6}-\frac{\beta\gamma A^3}{2}+\frac{3\gamma^2A^4}{128}=0 \tag{38}$$

From equation (38), the following expression for the nonlinear frequency of the multilayer plates composed of NHOPs is obtained:

$$\Omega_{NL}^{ST}=\sqrt{\frac{\left(\omega_L^{ST}\right)^2+\frac{3}{4}\gamma A^2+\sqrt{\left[\left(\omega_L^{ST}\right)^2+\frac{3}{4}\gamma A^2\right]^2+2\beta\gamma A^3-\frac{10\beta^2A^2}{3}-\frac{3\gamma^2A^4}{32}}}{2}} \tag{39}$$

The following expression is used for the dimensionless nonlinear frequency of multilayer plates composed of NHOPs

$$\bar{\Omega}_{NL}^{ST}=\Omega_{NL}^{ST}h\sqrt{\frac{\rho_0^{(k)}}{E_{11}^{0(k)}}} \tag{40}$$

The effect of geometric nonlinearity is found from the following expression:

$$\frac{\Omega_{NL}^{ST}}{\omega_L^{ST}}=\frac{1}{\sqrt{2}}\sqrt{1+\frac{3}{4}\frac{\gamma A^2}{\left(\omega_L^{ST}\right)^2}+\sqrt{\left[1+\frac{3}{4}\frac{\gamma A^2}{\left(\omega_L^{ST}\right)^2}\right]^2+\frac{1}{\left(\omega_L^{ST}\right)^4}\left(2\beta\gamma A^3-\frac{10\beta^2A^2}{3}-\frac{3\gamma^2A^4}{32}\right)}} \tag{41}$$

When transverse shear strains are ignored in the basic relations, appropriate formulas can be obtained in the framework of Kirchhoff-Love theory (KLT). In this case, Ω_{NL}^{KT}, $\bar{\Omega}_{NL}^{KT}$ and $\Omega_{NL}^{KT}/\omega_L^{KT}$ are used instead of Ω_{NL}^{ST}, $\bar{\Omega}_{NL}^{ST}$ and $\Omega_{NL}^{ST}/\omega_L^{ST}$.

5. Results and Discussion

5.1. Comparative examples

Three comparisons are made for the accuracy of the obtained formulas. When the calculations in the comparisons are made, vibration modes are not included in the tables for cases where the minimum values of the frequency parameter are obtained at $(m,n)=(1,1)$.

Example 1: In this example, the dimensionless frequency parameter values of the multilayer homogeneous orthotropic square plate arranged in (0º/90º/0º) in the framework of SDT and KLT for different a/h ratios are compared with the results obtained in the study of Aagaah et al. [45] that used finite element method (See, Table 1). The dimensionless frequency parameter is expressed as, $\omega_{1L}^{ST}=\omega_{L}^{ST}\dfrac{a^2}{h}\sqrt{\dfrac{\rho_0^{(k)}}{E_{22}^{0(k)}}}$. The following material properties are used in the comparisons:

$$E_{11}^{0(k)}=175\text{GPa}, E_{22}^{0(k)}=7\,\text{GPa},\ \nu_{12}^{(k)}=0.25, G_{12}^{0(k)}=G_{13}^{0(k)}=3.5\,\text{GPa},\ G_{12}^{0(k)}=1.4\,\text{GPa},\ \rho_0^{(k)}=1.$$

In this study, can be used instead of SDT when a/h=100. It can be seen from Table 1 that the dimensionless linear frequency parameter values obtained within the framework of SDT and KLT in this study are in good agreement with the results in the literature.

Example 2: Table 2 presents the variation of dimensionless frequency parameter $\omega_{1L}^{ST}=\omega_{L}^{ST}\dfrac{a^2}{h}\sqrt{\dfrac{\rho_0^{(k)}}{E_{22}^{0(k)}}}$ values of monolayer homogeneous orthotropic square and rectangular plates depending on the $E_{11}^{0(1)}/E_{22}^{0(1)}$ ratio for different a/b and a/h ratios using SDT, and it is compared with the results obtained by Thai and Kim[46] using the Levy type solution. The following material properties are used in numerical calculations: $E_{11}^{0(1)}/E_{22}^{0(1)}=3,10,\ 20,\ 30,40,50$; $G_{12}^{0(1)}=G_{13}^{0(1)}=0.5E_{11}^{0(1)}$, $G_{23}^{0(1)}=0.2E_{22}^{0(1)}$, $\nu_{12}^{(1)}=0.25$, $\rho_0^{(1)}=1$.

As seen in Table 2, the values obtained in this study are good agreement with the results of Thai and Kim [46].

Example 3: The nonlinear frequency to the linear frequency ratio ($\Omega_{NL}^{ST}/\omega_{L}^{ST}$) of multilayer homogeneous square plates with simply-supported boundary conditions for different A with $a/h=100$ are compared with the results of Singha and Daripa [47] that used the finite element method (See, Table 3). In our calculations is used the special case of the Eq. (39), that is, the case $\mu_i=0\,(i=1,2)$ is considered. The material properties for (0º/90º/0º/90º0º)-array plate are taken from Singha and Daripa [47] and are as follows:

$$E_{11}^{0(k)}/E_{22}^{0(k)}=40, G_{12}^{0(k)}/E_{22}^{0(k)}=G_{13}^{0(k)}/E_{22}^{0(k)}=0.6,\ G_{23}^{0(k)}/E_{22}^{0(k)}=0.5, \nu_{12}^{(k)}=0.25, \rho_0^{(k)}=1.$$

It is clearly seen from Table 3 that the numerical results obtained in this study for the $\Omega_{NL}^{ST}/\omega_{L}^{ST}$ ratio of multilayer plates are in good agreement with the finite element results of Ref. [47].

The comparison examples demonstrate that the results obtained in our study in both linear and nonlinear formulations are in agreement with the results in the literature and the formulas obtained are correct.

5.2. Specific analysis

The numerical results are performed for NL free vibration frequency of NH-orthotropic rectangular plates using Eqs. (39), (40) and (41). The non-homogeneity parameters for elasticity moduli and density are used as, $(\eta_1,\eta_2)=(+1,+1)$ or type NH_A, $(\eta_1,\eta_2)=(+1,0)$, or type NH_B and $(\eta_1,\eta_2)=(-1,0)$ or type NH_C and $(\eta_1,\eta_2)=(0,0)$ corresponds to homogeneous case (H). The properties of the homogeneous orthotropic material are taken from the study of Reddy [5]:

$E_{11}^{0(k)} = 2.069\times10^{11}$ Pa, $G_{12}^{0(k)} = G_{13}^{0(k)} = 6.9\times10^{9}$ Pa, $E_{22}^{0(k)} = 2.069\times10^{10}$ Pa, $G_{23}^{0(k)} = 4.14\times10^{9}$ Pa, $\rho_0^{(k)} = 1950\text{kg}/\text{m}^3$ and $\nu_{12}^{(k)} = 0.3$. For subsequent examples use the following characteristics: $a/b = 0.5,1.0,1.5,2.0$, $a/h = 15$, $A = 0,0.25,...,1.5$ by step 0.25 and $(m,n) = (1,1)$. Fig. 2 presents the cross-section of multilayer plates with different layer arrangements and numbers used in numerical analyses.

Table 4 presents the variation of dimensionless NL frequencies ($\bar{\Omega}_{NL}$) of homogeneous, single- and multi-layer plates within SDT and KLT depending on the dimensionless parameter A for different a/b. Table 4 will be used for comparison with Tables 5 and 6, where the variation of linear and NL frequencies of single layer and multilayer plates consisting of linear and quadratic non-homogeneous profiled layers within SDT and KLT depending on the a/b ratio is presented. The values corresponding to A=0, are linear frequency values and are the smallest values compared to NL frequency values in all tables.

Table 5 presents the variation of $\bar{\Omega}_{NL}$ of single layer and multilayer plates consisting of NH_A, NH_B and NH_C-linear profiled layers within SDT and KLT depending on the A with different a/b. When A and a/b ratios increase separately, there is the significant increase in dimensionless frequency values within the framework of both theories (see, Tables 4 and 5). In (0^o)-single layer plates, the influences of NH_A, NH_B and NH_C-linear profiles on the NL frequency remain constant at fixed values of A. While those effects remain constant for NH_A and NH_B-linear profiles in multilayer plates, they change for NH_C-linear profiles. From Tables 4 and 5, within SDT; At a/b=0.5, the influences of non-homogeneity on NL frequency in ($0^o/90^o/0^o$)-sequenced plates composed of NH_A (or NH_B) and NH_C-linear profile layers are (-5.21%) and (-5.13%), respectively, for A=0.25, while those effects reduce to (-2.74%) and (-2.56%), respectively, for A=1.5. At a/b=2.0, those effects are (-2.57%) and (-2.49%), respectively, for A=0.25, while those effects reduce to (-0.81%) and (-0.67%), respectively,

for A=1.5. As the a/b=1.0 and 1.5, the influences of NH-linear profiles on NL frequency vary between the influences when a/b=0.5 and 2. Therefore, just like the increase of the A ratio, the increase of the a/b ratio significantly reduces the influence of non-homogeneity on the NL frequency in NH-linear profiles. Moreover, the influences of NH_A and NH_B-linear profiles appear to be the same. When all layer arrangements are compared among themselves, it is seen that the most significant effect of the NH-linear profiles is on the plate with the order ($0^o/90^o/90^o/0^o$). When a/b increases from 0.5 to 2.0, the effect of the NH-linear profiles on the NL frequency in the ($0^o/90^o/90^o/0^o$)-array plate compared to the ($0^o/90^o/0^o$)-array plate is approximately 1% more for A=0.25. While it is significant, that effect difference decreases to 0.6% when A=1.5. The biggest difference in effect is between plates arranged in ($0^o/90^o/90^o/0^o$) and ($0^o/90^o$) and is seen to be around 3%.

At a/b =0.5, the effect of shear deformations on NL frequency is more evident in (0^o)-single layer plates with homogeneous and NH-linear profiles compared to multilayer plates, whereas, in multilayer plates starting with (90^o/…), the effect of shear deformations on the NL frequency is more pronounced as $a/b \geq 1$. It is observed that the layer arrangement in multilayer plates changes the influence of shear deformations compared to single layer plates and NH-linear profiles can be change that effect. For example at A=0.25, the most significant effect of shear deformations on the NL frequency in ($90^o/0^o/0^o/90^o$)-sequence plates is 1.9% in the homogeneous case and about 1.81% in the NH_A, NH_B and NH_C-linear profiles, as a/b =0.5, while those effects increase significantly, reaching 23.82% for the homogeneous case and approximately 22% for all NH-linear profiles, as a/b =2.0. Although at small values of A, the significant effect of shear deformations occurs in multilayer plates starting with (0^o/…)-sequences, when A increases, that effect occurs in multilayer plates starting with (90^o/…)-sequences.

Within the framework of SDT, when the a/b ratio increases from 0.5 to 1.0, the effect of the layer arrangement on the NL frequency reduces in NH-linear profile multilayer plates compared to (0^o) single layer plates, while it shows the significant increase when the a/b ratio increases from 1 to 2. Within the framework of SDT, the most significant effect of the layer arrangement on the NL frequency is in the ($90^o/0^o/90^o$)-array plates. For example, for the NH_A-linear profile at a/b =2 and when A=0.25 and 1.5, the alignment effect on the NL frequency is seen to be 116.7% and 114.1%, respectively. It is noted that the effect under consideration is also significant for all other layer alignments.

Table 6 presents the variation of $\bar{\Omega}_{NL}$ of single layer and multilayer plates consisting of NH_A, NH_B and NH_C-quadratic profiled layers within SDT and KLT depending on the A with different a/b ratio. In Figs. 3-6, the change of NL frequency values according to the A ratio for all layers is plotted, taking into account the values at a/b = 0.5 in Tables 4 and 6. When A and a/b ratios increase separately, there is the significant increase in dimensionless frequency values of plates consisting of quadratic non-homogeneous profiled layers within the framework of both theories. It is seen that from Tables 4 and 6, the effects of NH_A, NH_B and NH_C -quadratic profiles on the NL frequency in single layer and multi-layer plates are different at fixed A and have different effects. In the SDT framework, at a/b =0.5, the effect of NH_A, NH_B and NH_C-quadratic profiles on the NL frequency in ($0^o/90^o/90^o/0^o$)-sequenced plates is greater than all other arrangements and single layer plates and become (+2.95%), (+7.16%) and (-7.84%), respectively, as A=0.25, while those influences decrease and become (+2.56%), (+6.74%) and (-7.36%), respectively as A=1.5 (see. Figs. 3-6 also). At a/b=1.0 and a/b=1.5, the influences of NH-quadratic profiles on NL frequency continue to decrease, and at a/b=2.0 and for A=0.25 those effects are (+0.52%), (+4.6%) and (-4.93%), respectively, while for A =1.5 those effects decrease and become (-1.36%), (+2.66%) and (-2.77%), respectively.

Therefore, increasing the a/b ratio, as well as increasing the A ratio, significantly reduces the effect of non-homogeneity in quadratic profiles, and in some cases causes the non-homogeneity effect to disappear. In addition, unlike linear profiles, it is seen that the effects of NH_A and NH_B-quadratic profiles on the NL frequency are significantly different from each other.

For all the A, the influence of shear deformations on the NL frequency is more evident in (0^o)-single layer homogeneous and NH-quadratic profile plates compared to multilayer plates starting with (0^o/…)-sequences. While for $A \le 0.25$, the shear deformations effect is more evident in multilayer plates starting with (90^o/…)-sequences for $A > 0.25$, the that effect begins to become more evident in multilayer plates starting with (90^o/…)-sequences and as the A increases the prominence begins to increase further. While the change in layer arrangement and number rises or reduces the effect of shear deformations on NL frequency compared to (0^o)-single layer plate, the NH-quadratic profiles can also increase or decrease that effect. For example, in plates consisting of layers with NH_A and NH_B-quadratic profiles, the effect of shear deformations on the NL frequency greater than in the homogeneous case, while those effect is lower in the NH_C-quadratic profile compared to the homogeneous case. For all profiles starting with (0^o/…)-sequences, the effect of shear deformations on the NL frequency first decreases and rises after reaching the minimum value, when the a/b ratio increases from 0.5 to 2, while for profiles starting with (90^o/...)-sequences, as the a/b ratio increases, the influence of the shear deformations continuously rises. The most significant effects of shear deformations occur in the ($90^o/0^o/90^o$)-aligned plate with 1.86%, %2.13, 2.04% and 1.5% for homogeneous, NH_A-, NH_B- and NH_C-quadratic profiles, respectively for a/b=0.5, while those influences are more effective and are 16.85%, 18.21%, 18.2% and 15.37%, respectively, for a/b=2 and at A=0.25. It is noted that as the A=1.5, those effects are reduced by approximately half. Although at small values of A, the significant effects of shear deformations occur in multilayer plates

starting with (0º/…)-array, that effect occurs in multilayer plates starting with (90º/…)-array, when A increases.

The variations of $\Omega_{NL}^{ST}/\omega_L^{ST}$ and $\Omega_{NL}^{KT}/\omega_L^{KT}$ for (0º/90º/90º/0º) -array plates composed of H and NH_A-linear and quadratic profiles within SDT and KLT against the A with different a/h are illustrated in Figs. 7 and 8. As can be seen, when the A and a/b ratio increase, the $\Omega_{NL}^{ST}/\omega_L^{ST}$ and $\Omega_{NL}^{KT}/\omega_L^{KT}$ increase significantly. The influence of shear deformations and material gradient on the $\Omega_{NL}^{ST}/\omega_L^{ST}$ increases with the increase of the A for all a/b in the (0º/90º/90º/0º)-array plate for linear and quadratic profiles. When the values of the Ω_{NL}/ω_L ratio are compared within the framework of KLT and SDT, it is more evident in SDT. When the a/b ratio increases from 0.5 to 2, the $\Omega_{NL}^{ST}/\omega_L^{ST}$ ratio increases from 0.1% to 0.68% at A =0.25, whereas that effect increases from 2.72% to 7.5% at A=1.5. When the $\Omega_{NL}^{ST}/\omega_L^{ST}$ for NH-linear and NH-quadratic profiles is compared, it can be seen that the NH-quadratic profile is more effective. The influence of non-homogeneity on the $\Omega_{NL}^{ST}/\omega_L^{ST}$ ratio increases up to 3.1% in the NH_A-linear profiled plate for a/b=0.5, while that effect remains 0.44% in the NH_A-quadratic profiled plate, while those effects are 2.1% and 2.05%, respectively for a/b=2.

6. Conclusions

In this study, the Poincaré-Lindstedt method is applied for the first time to the solution of NL vibration problem of multilayer plates consisting of NHOLs within SDT. By using von-Karman type nonlinearity, the basic relations of multilayer plates consisting of NHOLs are established and then NL equations of motion are derived. Then, NL-PDEs are reduced to NL-ODE depending on the deflection amplitude by means of the Galerkin method. The solution of NL-ODE is performed by the modified Poincaré -Lindstedt method, yielding new amplitude dependent expressions for NL frequency, and for the ratio of NL/L frequency ratio for

multilayer plates composed of NHOLs. Finally, detailed parametric studies are carried out to gain insight into the effects of various factors such as shear strains, non-homogeneity, number and array of layers on the NL frequency and NL/L frequency ratio for different rectangular plate characteristics.

References

[1] Reissner E. The effect of transverse shear deformation on the bending of elastic plates. ASME J Appl Mech 1945; 12: 69–77.

[2] Mindlin RD. Influence of rotatory inertia and shear on flexural motions of isotropic, elastic plates. ASME J Appl Mech 1951; 181: 31–8.

[3] Ambartsumian SA. Theory of Anisotropic Plates; Strength, Stability, Vibration. Technomic Publishing Company, Stamford, 1970.

[4] Qatu MS. Vibration of Laminated Shells and Plates. San Diego, CA: Elsevier, 2004.

[5] Reddy JN. Mechanics of Laminated Composite Plates and Shells: Theory and Analysis. 2nd ed. CRC Press, New-York, 2004.

[6] Kurpa LV, Timchenko GN. Studying the free vibrations of multilayer plates with a complex planform. Int Appl Mech 2006;42:103-9.

[7] Singha, M.K., Daripa R. Nonlinear vibration of symmetrically laminated composite skew plates by finite element method. Int J Non-Lin Mech 2007; 429:1144-52.

[8] Amabili M, Karazis K, Khorshidi K. Nonlinear vibrations of rectangular laminated composite plates with different boundary conditions. Int J Struct Stab Dyn 2011; 1104: 673-95.

[9] Pandey R, Upadhyay AK, Shukla KK, Jain A. Nonlinear dynamic response of elastically supported laminated composite plates. Mech Adv Mater Struct 2012;19(6): 397–420.

[10] Chen JE, Zhang W, Guo XY, Sun M. Theoretical and experimental studies on nonlinear oscillations of symmetric cross-ply composite laminated plates. Nonlin Dyn 2013;73(3): 1697-714.

[11] Shi P, Dong CY. A refined hyperbolic shear deformation theory for nonlinear bending and vibration isogeometric analysis of laminated composite plates. Thin-Walled Struct 2022;174:109031.

[12] Nguyen VH, Nguyen TK, Thanh CD. Geometrically nonlinear analysis of laminated composite plates using cell- and edge-based smoothing MITC3 Finite Elements. Int J Computat Meth 2022;19 (1): 2150053.

[13] Lewandowski R, Litewka P. Nonlinear harmonic vibrations of laminate plates with VE layers using refined zig-zag theory. Part 2-Numerical solution. Compos Struct 2023; 319:117062.

[14] Daneshkhah E, Carrera E. Advanced finite elements for geometrically nonlinear analysis of rectangular plates under various in-plane loadings accounting for the boundary conditions of the stiffeners. J Eng Mech 2023;149 (3):04022117.

[15] Motamedi AR, Noormohammadi N, Boroomand B. A novel Trefftz-based meshfree method for free vibration and buckling analysis of thin arbitrarily shaped laminated composite and isotropic plates. Computers & Math Appl 2023;145:318-40.

[16] Grigorenko YM, Vasilenko AT. Static problems for anisotropic inhomogeneous shells [in Russian], Nauka, Moscow, 1992.

[17] Pan E. Exact solution for functionally graded anisotropic elastic composite laminates J Compos Mater 2003;37 (21): 1903-20.

[18] Sofiyev AH, Schnack E. The buckling of cross-ply laminated non-homogeneous orthotropic composite conical thin shells under a dynamic external pressure Acta Mech 2003;162(1-4): 29-40.

[19] Ootao Y, Tanigawa Y. Three-dimensional solution for transient thermal stresses of an orthotropic functionally graded rectangular plate. Compos Struct 2007; 80(1): 10-20.

[20] Grigorenko YM, Grigorenko AY. Static and dynamic problems for anisotropic inhomogeneous shells with variable parameters and their numerical solution. Int Appl Mech 2013;49 (2): 123-93.

[21] Awrejcewicz J, Krysko VA. Theory of Non-Homogeneous Shells. Chapter in the Book; Chaos in Structural Mechanics, Springer-Verlag, 2008:15-40.

[22] Wang YM, Tarn JQ. A 3-Dimensional analysis of anisotropic inhomogeneous and laminated plates. Int J Solids Struct 1994; 31(4): 497-515.

[23] Fares ME, Zenkour AM. Buckling and free vibration of non-homogeneous composite cross-ply laminated plates with various plate theories. Compos Struct 1999;44(4):279-87.

[24] Spencer AJM. Three-dimensional elasticity solutions for anisotropic and inhomogeneous plates and shells. Proceed Int Conf Int Meth Sci Eng 2002;1:233-44.

[25] Chen WQ, Lee KY, Ding HJ. On free vibration of non-homogeneous transversely isotropic magneto-electro-elastic plates. J Sound Vib 2005; 279 (1-2):237-51.

[26] Kuo SY, Shiau LC. Buckling and vibration of composite laminated plates with variable fiber spacing. Compos Struct 2009; 90(2):196-200.

[27] Orakdögen E, Küçükarslan S, Sofiyev A, Omurtag MH. Finite element analysis of functionally graded plates for coupling effect of extension and bending. Meccanica 2010; 45(1): 63-72.

[28] Zerin Z. On the vibration of laminated nonhomogeneous orthotropic shells. Meccanica 2013: 48(7):1557-72.

[29] Sofiyev AH, Kuruoglu N. Combined influences of shear deformation, rotary inertia and heterogeneity on the frequencies of cross-ply laminated orthotropic cylindrical shells. Compos Part B: Eng 2014; 66:500-10.

[30] Flores FG, Oller S, Nallim LG. On the analysis of non-homogeneous laminates using the refined zigzag theory. Compos Struct 2018;204:791-802.

[31] Haciyev VC, Sofiyev AH, Kuruoglu N. Free bending vibration analysis of thin bidirectionally exponentially graded orthotropic rectangular plates resting on two-parameter elastic foundations. Compos Struct 2018;184: 372-77.

[32] Haciyev VC, Sofiyev AH, Kuruoglu N. On the free vibration of orthotropic and inhomogeneous with spatial coordinates plates resting on the inhomogeneous viscoelastic foundation**.** Mech Adv Mater Struct 2019;2610: 886-97.

[33] Bacciocchi, M, Tarantino AM. Natural frequency analysis of functionally graded orthotropic cross-ply plates based on the finite element method. Math Computat Appl 2019;24(2): 52

[34] Sofiyev AH. Application of the first order shear deformation theory to the solution of free vibration problem for laminated conical shells. Compos Struct 2018;188:340-46.

[35] Bouazza M, Zenkour AM. Vibration of inhomogeneous fibrous laminated plates using an efficient and simple polynomial refined theory. J Computat Appl Mech 2021; 52 (2): 233-45.

[36] Song YY, Li QH, Xue K. An analytical method for vibration analysis of arbitrarily shaped non-homogeneous orthotropic plates of variable thickness resting on Winkler-Pasternak foundation. Compos Struct 2022; 296:115885.

[37] Ribeiro P, Akhavan H. Non-linear vibrations of variable stiffness composite laminated plates. Compos Struct 2012; 94(8):2424-32.

[38] Awrejcewicz J, Krysko AV, Mitskevich SA, Zhigalov MV, Krysko VA. Nonlinear dynamics of heterogeneous shells Part 1. Statics and dynamics of heterogeneous variable stiffness shells. Int J Non-Lin Mech 2021;130:103669.

[39] Krysko AV, Awrejcewicz J, Bodyagina KS, Krysko VA. Mathematical modeling of planar physically nonlinear inhomogeneous plates with rectangular cuts in the three-dimensional formulation. Acta Mech 2021; 232 (12): 4933-50.

[40] Awrejcewicz J, Kurpa L, Shmatko T. Linear and nonlinear free vibration analysis of laminated functionally graded shallow shells with complex plan form and different boundary conditions. Int J Non Linear Mech 2018;107:161-69.

[41] Gupta A, Pradyumna S. Geometrically nonlinear dynamic analysis of variable stiffness composite laminated and sandwich shell panels. Thin Walled Struct 2022;173:109021.

[42] Ribeiro P, Antunes AM, Akhavan H, Rodrigues JD. Non-linear forced vibrations of variable stiffness plates on elastic supports. Mech Adv Mater Struct 2023;30(20):4246-63.

[43] Volmir AS. The nonlinear dynamics of plates and shells. Science Edition, Moscow 1972.

[44] Hashemi S, Jafari AA. An analytical solution for nonlinear vibrations analysis of functionally graded plate using modified Lindstedt–Poincare method. Int J Appl Mech 2020;1201: 2050003.

[45] Aagaah MR, Mahinfalah M, Jazar GN. Natural frequencies of laminated composite plates using third order shear deformation theory. Compos Struct 2006;72: 273–79.

[46] Thai HT, Kim SE. Levy-type solution for free vibration analysis of orthotropic plates based on two variable refined plate theory. Appl Math Model 2012;36(8):3870–82.

[47] Singha MK, Daripa R. Nonlinear vibration and dynamic stability analysis of composite plates. J Sound Vib 2009;328: 541-54.

Appendix A

Here L_{ij} are differential operators and are defined as follows:

$$
\begin{aligned}
&L_{11}(\Psi)=h\left[(s_{11}-s_{31})\frac{\partial^4}{\partial x^2\partial y^2}+s_{12}\frac{\partial^4}{\partial x^4}\right],\ L_{12}(W)=\rho_1\frac{\partial^4}{\partial x^2\partial t^2}-s_{13}\frac{\partial^4}{\partial x^4}-\left(s_{14}+s_{32}\right)\frac{\partial^4}{\partial x^2\partial y^2},\\
&L_{13}(\varphi_1)=s_{15}\frac{\partial^3}{\partial x^3}+s_{35}\frac{\partial^3}{\partial x\partial y^2}-\Delta_3\frac{\partial}{\partial x}-\rho_2\frac{\partial^3}{\partial x\partial t^2},\ L_{14}(\varphi_2)=s_{18}\frac{\partial^3}{\partial x^2\partial y}+s_{38}\frac{\partial^3}{\partial x^2\partial y},\\
&L_{21}(\Psi)=h\left[s_{21}\frac{\partial^4}{\partial y^4}+\left(s_{22}-s_{31}\right)\frac{\partial^4}{\partial x^2\partial y^2}\right],L_{22}(W)=-\left(s_{32}+s_{23}\right)\frac{\partial^4}{\partial x^2\partial y^2}-s_{24}\frac{\partial^4}{\partial y^4}+\rho_1\frac{\partial^4}{\partial x^2\partial t^2},\\
&L_{23}(\varphi_1)=s_{35}\frac{\partial^3}{\partial x\partial y^2}+s_{25}\frac{\partial^3}{\partial x\partial y^2},\ L_{24}(\varphi_2)=s_{38}\frac{\partial^3}{\partial x^2\partial y}+s_{28}\frac{\partial^3}{\partial y^3}-\Delta_4\frac{\partial}{\partial y}-\rho_3\frac{\partial^3}{\partial y\partial t^2},\\
&L_{31}(\Psi)=0,\ L_{32}(W)=-\overline{\rho}\frac{\partial^2}{\partial t^2},\ L_{33}(\varphi_1)=\Delta_3\frac{\partial}{\partial x},\\
&L_{34}(\varphi_2)=\Delta_4\frac{\partial}{\partial y},\ L_{35}(\Psi,W)=h\left(\frac{\partial^2}{\partial y^2}\frac{\partial^2}{\partial x^2}-2\frac{\partial^2}{\partial x\partial y}\frac{\partial^2}{\partial x\partial y}+\frac{\partial^2}{\partial x^2}\frac{\partial^2}{\partial y^2}\right).
\end{aligned}
\tag{A.1}
$$

and

$$
\begin{aligned}
&L_{41}(\Psi)=h\left[r_{11}\frac{\partial^4}{\partial y^4}+\left(r_{12}+r_{21}+r_{31}\right)\frac{\partial^4}{\partial x^2\partial y^2}+r_{22}\frac{\partial^4}{\partial x^4}\right],\\
&L_{42}(W)=-r_{23}\frac{\partial^4}{\partial x^4}-\left(r_{24}+r_{13}-r_{32}\right)\frac{\partial^4}{\partial x^2\partial y^2}-r_{14}\frac{\partial^4}{\partial y^4},\\
&L_{43}(\varphi_1)=r_{25}\frac{\partial^3}{\partial x^3}+r_{15}\frac{\partial^3}{\partial x\partial y^2}+r_{35}\frac{\partial^3}{\partial x\partial y^2},\ L_{44}(\varphi_2)=r_{28}\frac{\partial^3}{\partial x^2\partial y}+r_{38}\frac{\partial^3}{\partial x^2\partial y}+r_{18}\frac{\partial^3}{\partial y^3},\\
&L_{45}(W,W)=\frac{\partial^2}{\partial x^2}\frac{\partial^2}{\partial y^2}-\left(\frac{\partial^2}{\partial x\partial y}\right)^2.
\end{aligned}
\tag{A.2}
$$

Among these symbols, the following definitions apply:

$$
\begin{aligned}
&s_{11}=A_{11}^1r_{11}+A_{12}^1r_{21},\ s_{12}=A_{11}^1r_{12}+A_{12}^1r_{11},\ s_{13}=A_{11}^1r_{13}+A_{12}^1r_{23}+A_{11}^2,\ s_{14}=A_{11}^1r_{14}+A_{12}^1r_{24}+A_{12}^2,\\
&s_{15}=A_{11}^1r_{15}+A_{12}^1r_{25}+A_{15}^1,\ s_{18}=A_{11}^1r_{18}+A_{12}^1r_{28}+A_{18}^1,\ s_{21}=A_{21}^1r_{11}+A_{22}^1r_{21},\ s_{22}=A_{21}^1r_{12}+A_{22}^1r_{22},\\
&s_{23}=A_{21}^1r_{13}+A_{22}^1r_{23}+A_{21}^2,\ s_{24}=A_{21}^1r_{14}+A_{22}^1r_{24}+A_{22}^2,\ s_{25}=A_{21}^1r_{15}+A_{22}^1r_{25}+A_{25}^1,\\
&s_{28}=A_{21}^1r_{18}+A_{22}^1r_{28}+A_{28}^1,\ s_{31}=A_{66}^1r_{35},\ s_{32}=A_{66}^1r_{32}+2A_{66}^2,s_{35}=A_{35}^1-A_{66}^1r_{35},\ s_{38}=A_{38}^1-A_{66}^1r_{38},
\end{aligned}
\tag{A.3}
$$

where

$$
\begin{aligned}
&r_{11}=\frac{A_{22}^{0}}{\overline{A}},\ r_{12}=-\frac{A_{12}^{0}}{\overline{A}},\ r_{13}=\frac{A_{12}^{0}A_{21}^{1}-A_{11}^{1}A_{22}^{0}}{\overline{A}},\ r_{14}=\frac{A_{12}^{0}A_{22}^{1}-A_{12}^{1}A_{22}^{0}}{\overline{A}},\ r_{15}=\frac{A_{25}^{0}A_{12}^{0}-A_{15}^{0}A_{22}^{0}}{\overline{A}},\\
&r_{18}=\frac{A_{28}^{0}A_{12}^{0}-A_{18}^{0}A_{22}^{0}}{\overline{A}},\ r_{21}=-\frac{A_{21}^{0}}{\overline{A}},\ r_{22}=\frac{A_{11}^{0}}{\overline{A}},\ r_{23}=\frac{A_{11}^{1}A_{21}^{0}-A_{21}^{1}A_{11}^{0}}{\overline{A}},\ r_{24}=\frac{A_{12}^{1}A_{21}^{0}-A_{22}^{1}A_{11}^{0}}{\overline{A}},\\
&r_{25}=\frac{A_{15}^{0}A_{21}^{0}-A_{25}^{0}A_{11}^{0}}{\overline{A}},\ r_{28}=\frac{A_{18}^{0}A_{21}^{0}-A_{28}^{0}A_{11}^{0}}{\overline{A}},\ r_{31}=\frac{1}{A_{66}^{0}},\ r_{32}=-\frac{2A_{66}^{1}}{A_{66}^{0}},r_{35}=\frac{A_{35}^{0}}{A_{66}^{0}},\ r_{38}=\frac{A_{38}^{0}}{A_{66}^{0}},\\
&\overline{A}=A_{11}^{0}A_{22}^{0}-A_{12}^{0}A_{21}^{0}
\end{aligned}
\tag{A.4}
$$

in which

$$
\begin{aligned}
&A_{ij}^{l_1}=\sum_{k=1}^{N}\int_{z_{k-1}}^{z_k}\overline{E}_{ijZ}^{(k)}z^{l_1}\mathrm{d}z\,(i,j=1,2,6),A_{15}^{l_2}=\sum_{k=1}^{N}\int_{z_{k-1}}^{z_k}\overline{E}_{11Z}^{(k)}\Delta_{1z}^{(k)}z^{l_2}\mathrm{d}z,\ A_{18}^{l_2}=\sum_{k=1}^{N}\int_{z_{k-1}}^{z_k}\overline{E}_{12Z}^{(k)}\Delta_{2z}^{(k)}z^{l_2}\mathrm{d}z,\\
&A_{25}^{l_2}=\sum_{k=1}^{N}\int_{z_{k-1}}^{z_k}\overline{E}_{21Z}^{(k)}\Delta_{1z}^{(k)}z^{l_2}\mathrm{d}z,A_{28}^{l_2}=\sum_{k=1}^{N}\int_{z_{k-1}}^{z_k}\overline{E}_{22Z}^{(k)}\Delta_{2z}^{(k)}z^{l_2}\mathrm{d}z,\ A_{35}^{l_2}=\sum_{k=1}^{N}\int_{z_{k-1}}^{z_k}\overline{E}_{66Z}^{(k)}\Delta_{1z}^{(k)}z^{l_2}\mathrm{d}z,\\
&A_{35}^{l_2}=\sum_{k=1}^{N}\int_{z_{k-1}}^{z_k}\overline{E}_{66Z}^{(k)}\Delta_{2z}^{(k)}z^{l_2}\mathrm{d}z,\ \left(l_1=0,1,2;\ l_2=0,1\right),\\
&\Delta_{j_1}=\sum_{k=1}^{N}\int_{z_{k-1}}^{z_k}\frac{\mathrm{d}f_i^{(k)}}{\mathrm{d}z}\mathrm{d}z,\ (j_1=3,4),\ -\frac{h}{2}+\frac{(k-1)h}{N}\le z\le-\frac{h}{2}+\frac{kh}{N}\ .
\end{aligned}
\tag{A.5}
$$

Appendix B

Here, the coefficients $u_{ij}(i=1,2,3,\ j=1,2,...,5)$ are described as

$$
\begin{aligned}
&u_{11}=J_{03}h\left[(s_{11}-s_{31})\eta_1{}^2\eta_2{}^2+s_{12}\eta_1{}^4\right]q_{11}-s_{13}\eta_1{}^4-\left(s_{14}+s_{32}\right)\eta_1{}^2\eta_2{}^2,\\
&u_{11}^{NL}=-hs_{12}\frac{64J_{01}}{3ab}\frac{\eta_1{}^3}{\eta_2}\left[1-(-1)^m-(-1)^n+(-1)^{m+n}\right],\\
&u_{12}=s_{15}\eta_1{}^3+s_{35}\eta_1\eta_2{}^2+\Delta_3\eta_1,\ u_{13}=(s_{18}+s_{38})\eta_1{}^2\eta_2,\\
&u_{21}=\eta_2{}^2\left[q_{11}hJ_{03}\left[s_{21}\eta_2{}^2+(s_{22}-s_{31})\eta_1{}^2\right]-\left(s_{32}+s_{23}\right)\eta_1{}^2-s_{24}\eta_2{}^2\right],\\
&u_{21}^{NL}=-s_{21}h\frac{64J_{02}}{3a^2}\frac{\eta_2{}^3}{\eta_1}\left[1-(-1)^m-(-1)^n+(-1)^{m+n}\right],\ u_{22}=(s_{25}+s_{35})\eta_1\eta_2{}^2,\\
&u_{23}=\eta_2\left(s_{28}\eta_2{}^2+s_{38}\eta_1{}^2+\Delta_4\right),u_{31}=0,\ u_{32}=2\eta_1{}^2\eta_2h\left(J_{01}+J_{02}\right),\\
&u_{33}=\Delta_3\eta_1,\ u_{34}=\Delta_4\eta_2,\ u_{31}^{NL}=-\frac{8h\eta_1\eta_2q_{11}J_{03}}{3ab}\left[1-(-1)^m-(-1)^n+(-1)^{m+n}\right].
\end{aligned}
\tag{B.1}
$$

where

$$
J_{01}=\frac{q_{14}}{32\eta_1{}^4q_3},\ J_{02}=\frac{q_{14}}{32\eta_2{}^4q_1},\ J_{03}=\frac{1}{q_1\eta_2{}^4+q_2\eta_2{}^2\eta_1{}^2+q_3\eta_1{}^4}
\tag{B.2}
$$

FIGURE AND TABLE CAPTIONS

Fig. 1. Geometry and coordinate system and cross section of multilayer plate

Fig.2. Cross-section of multilayer plate with different layer arrangements and numbers

Fig. 3. Variation of $\bar{\Omega}_{NL}^{ST}$ for (0º), (0º/90º) and (0º/90º/0º) -array plates composed of H and NH-quadratic profiles within SDT against the A with $a/b = 0.5$

Fig. 4. Variation of $\bar{\Omega}_{NL}^{KT}$ for (0º), (0º/90º) and (0º/90º/0º) -array plates composed of H and NH-quadratic profiles within KLT against the A with $a/b = 0.5$

Fig. 5. Variation of $\bar{\Omega}_{NL}^{ST}$ for (90º/0º/90º), (0º/90º/90º/0º) and (90º/0º/0º/90º) -array plates composed of H and NH-quadratic profiles within SDT against the A with $a/b = 0.5$

Fig. 6. Variation of $\bar{\Omega}_{NL}^{KT}$ for (90º/0º/90º), (0º/90º/90º/0º) and (90º/0º/0º/90º) -array plates composed of H and NH-quadratic profiles within KLT against the A with $a/b = 0.5$

Fig. 7. Variation of $\Omega_{NL}^{ST} / \omega_L^{ST}$ for (0º/90º/90º/0º) -array plates composed of H and NH_A-linear and quadratic profiles within SDT against the A with different a/b

Fig. 8. Variation of $\Omega_{NL}^{KT} / \omega_L^{KT}$ for (0º/90º/90º/0º) -array plates composed of H and NH-linear and quadratic profiles within KLT against the A with different a/b

Table 1

Comparison of dimensionless frequency parameters values of multilayer orthotropic square plates arranged in (0º/90º/0º) in the framework of SDT and KLT.

Table 2

Comparison of dimensionless frequency parameter of orthotropic plates using SDT with the results of Thai and Kim [46]

Table 3

Comparison of the nonlinear frequency to the linear frequency ratio of multilayer homogeneous square plates with the results of Ref. [47].

Table 4

Variation of $\bar{\Omega}_{NL}$ for single layer and multilayer homogenous plates within SDT and KLT versus A with different a / b

Table 5

Variation of $\bar{\Omega}_{NL}$ for single layer and multilayer plates consisting of linear non-homogeneous profiled layers within SDT and KLT versus A with different a / b ratio

Table 6

Variation of $\bar{\Omega}_{NL}$ for single layer and multilayer plates consisting of quadratic non-homogeneous profiled layers within SDT and KLT versus A with different a / b ratio

FIGURE 1

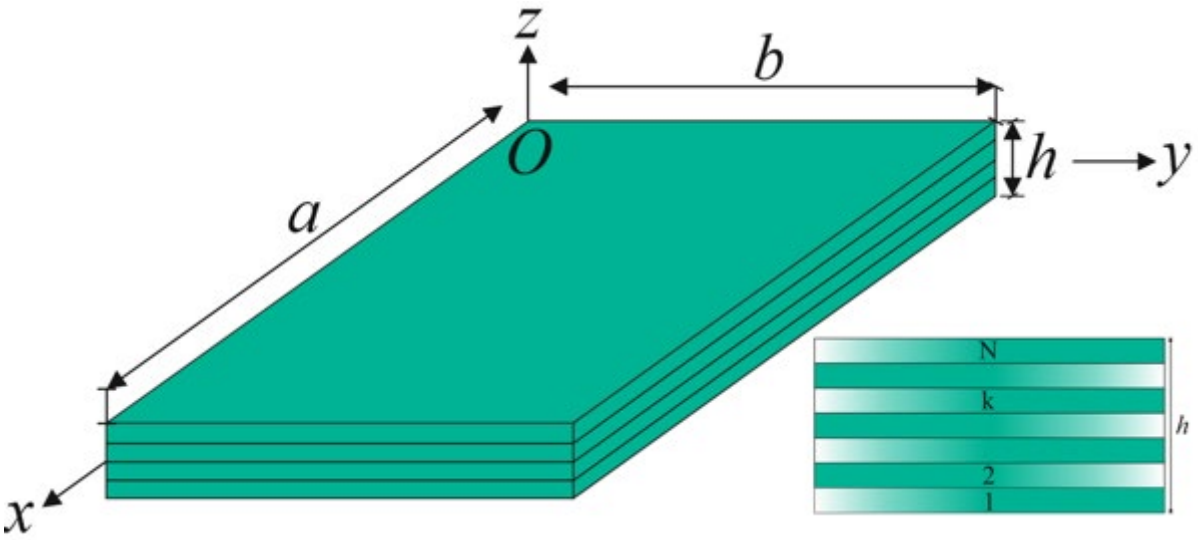

FIGURE 2

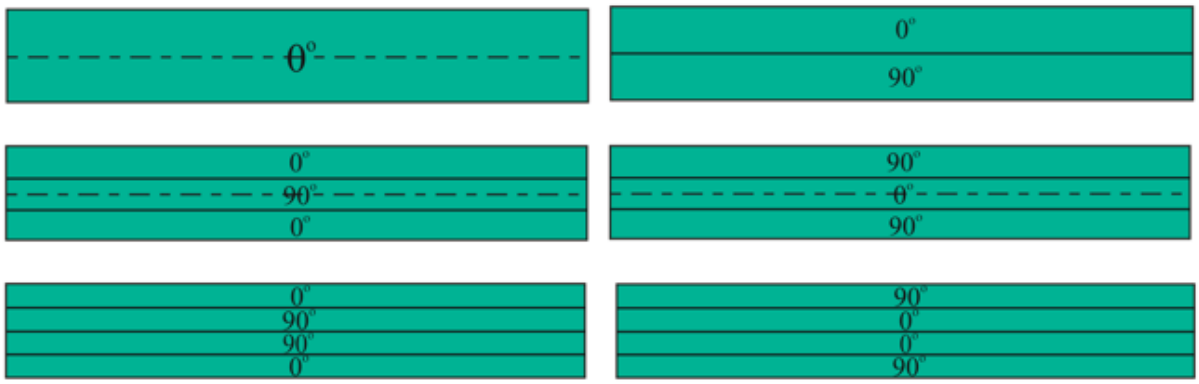

FIGURE 3

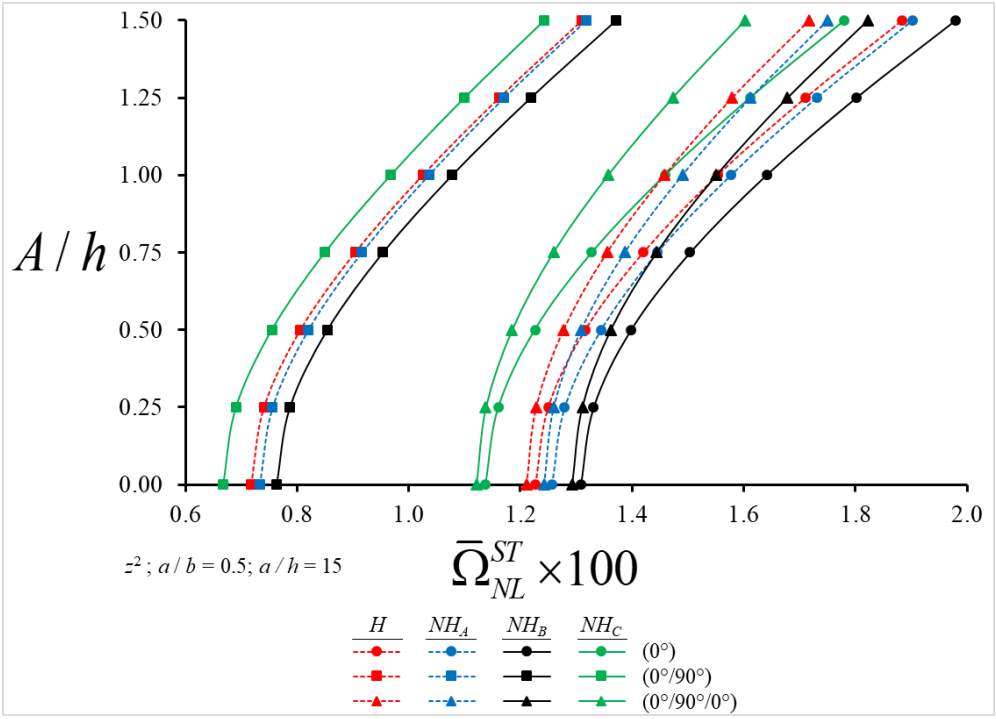

FIGURE 4

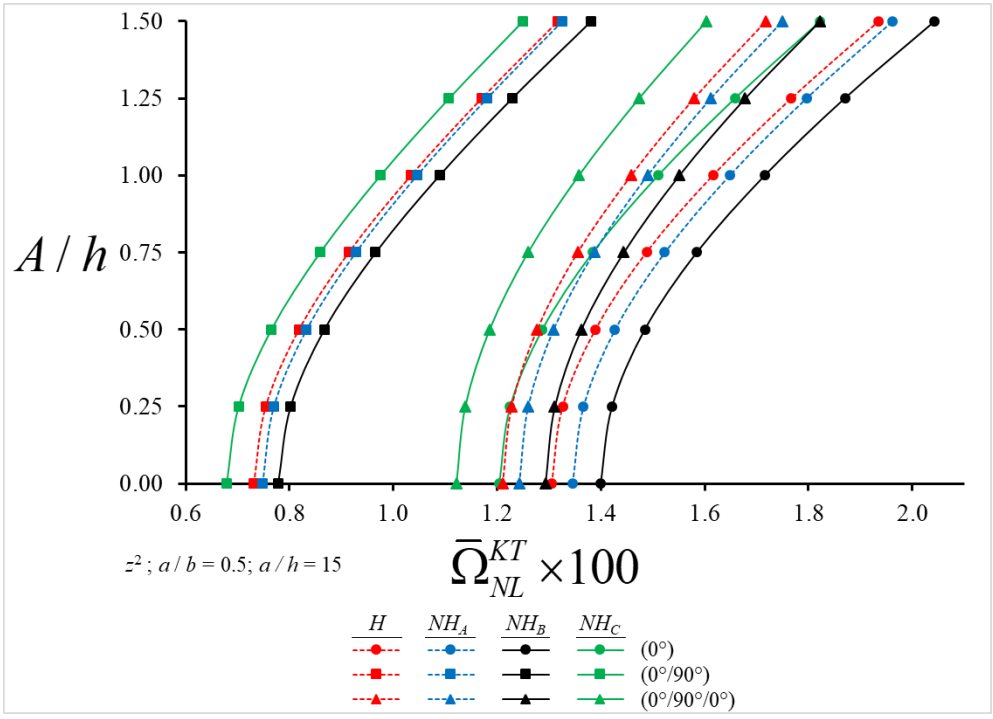

FIGURE 5

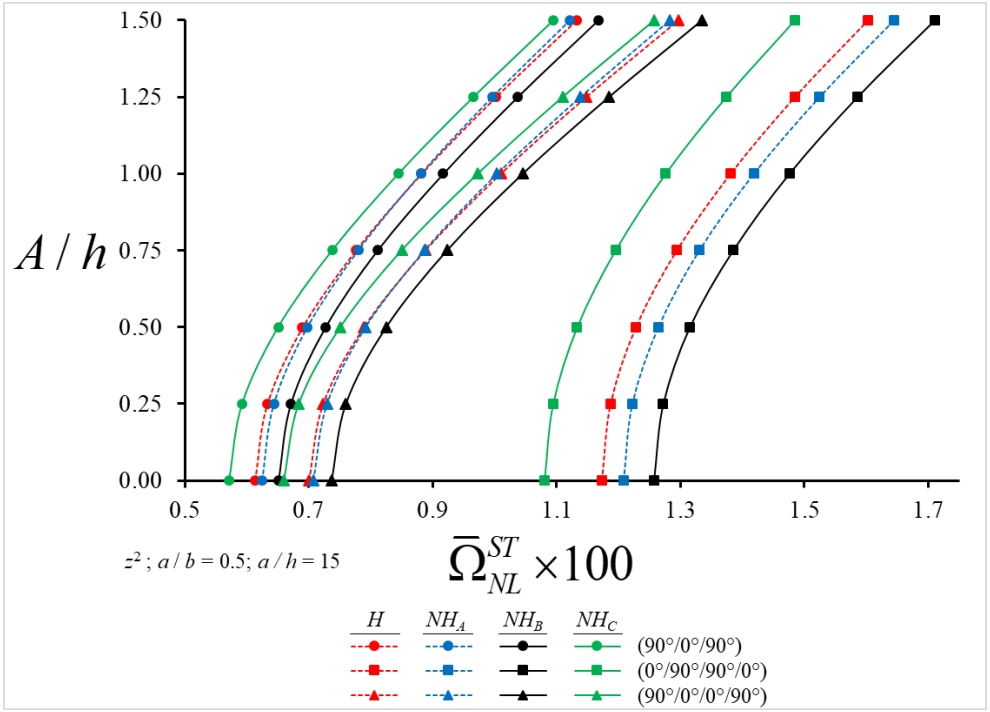

FIGURE 6

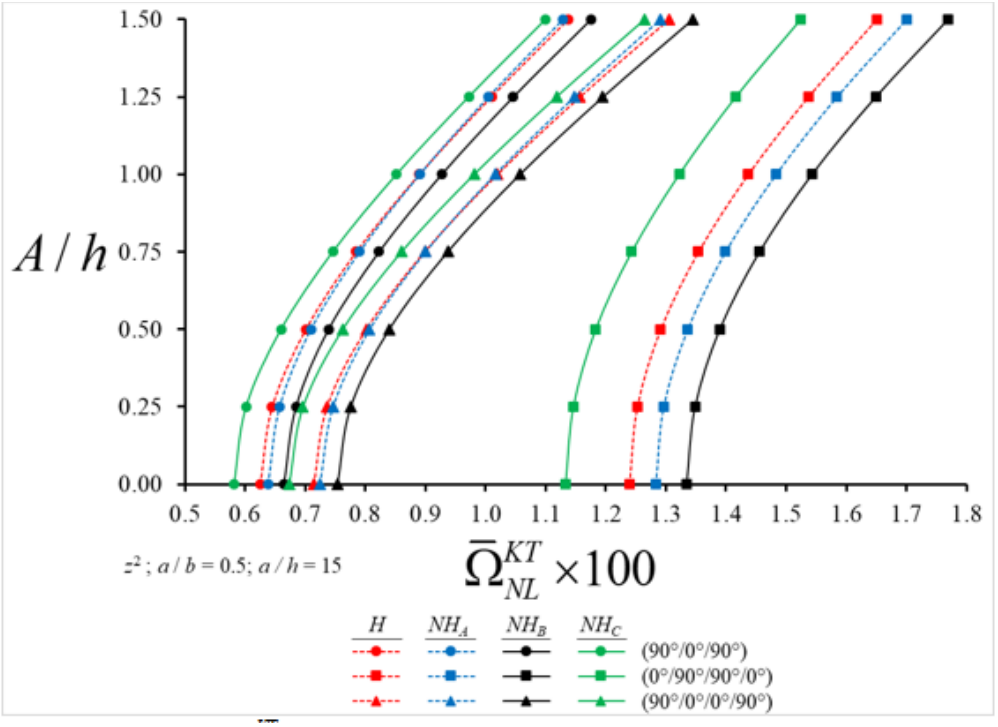

FIGURE 7

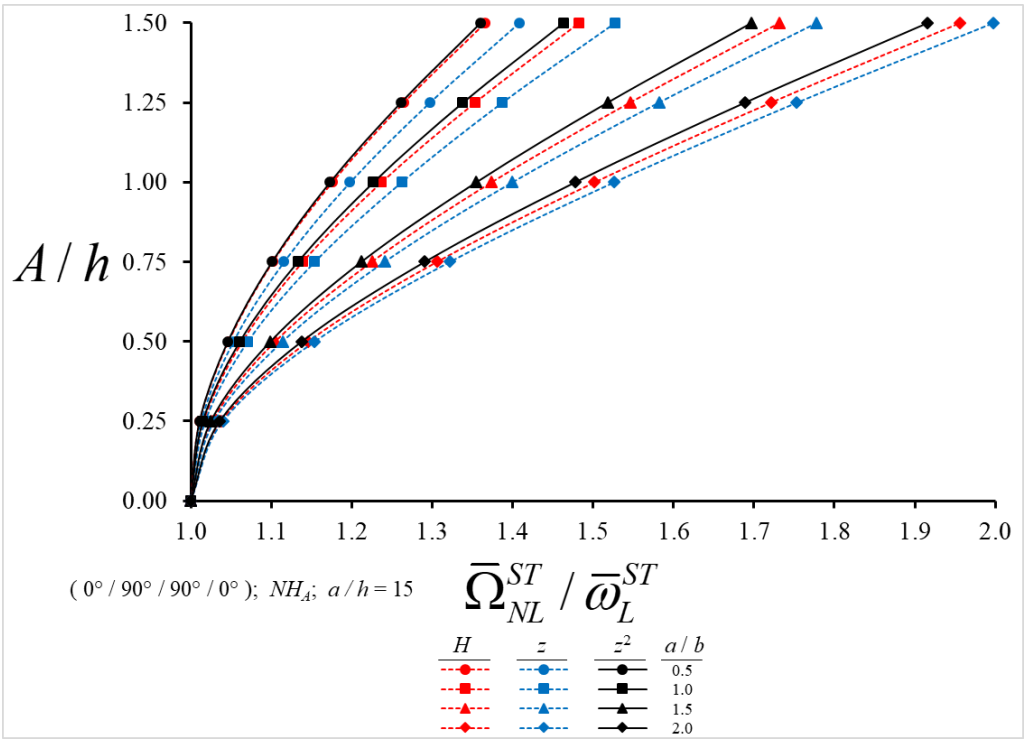

FIGURE 8

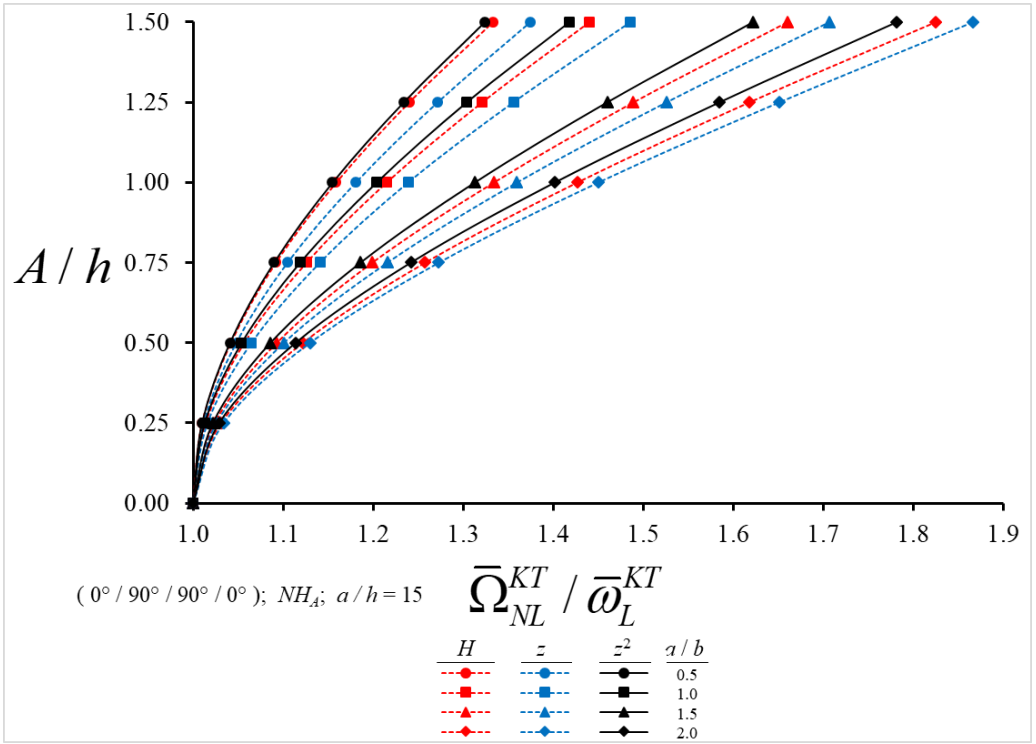

TABLE 1

	ω_{1L}^{ST}		
a/h	20	50	100
	(0º/90º/0º)		
Present study	14.422	15.089	15.193
Aagaah et al. [45]	14.004	14.906	15.041
	(0º/90º/0º/90º)		
Present study	14.488	15.102	15.196
Aagaah et al. [45]	14.032	14.936	15.071

TABLE 2

ω_{1L}^{ST}							
Thai and Kim [46]							
a/b	a/h	$E_{11}^{0(1)} / E_{22}^{0(1)}$					
		3	10	20	30	40	50
0.5	20	5.4685	9.1141	12.4009	14.7974	16.7105	18.3073
	50	5.5126	9.3044	12.8804	15.6246	17.9239	19.9333
1.0	20	7.2194	10.2349	13.2676	15.5845	17.4839	19.1002
	50	7.3012	10.4530	13.7360	16.3474	18.5726	20.5377
2.0	20	14.9772	16.5030	18.4742	20.2036	21.7468	23.1427
	50	15.3796	17.0294	19.1992	21.1436	22.9151	24.5504
Present study							
0.5	20	5.4639	9.0630	12.2432	14.5124	16.2887	17.7448
	50	5.5119	9.2957	12.8519	15.5700	17.8386	19.8136
1.0	20	7.2113	10.1763	13.0594	15.1856	16.8742	18.2698
	50	7.2999	10.4430	13.6982	16.2709	18.4496	20.3621
2.0	20	14.9231	16.4426	18.2813	19.7914	21.0621	22.1517
	50	15.3706	17.0195	19.1641	21.0635	22.7750	24.3383

TABLE 3

	$\Omega_{NL}^{ST} / \omega_{L}^{ST}$	
A	Present study	Singha and Daripa [47]
0.2	1.01044	1.01057
0.4	1.04105	1.04169
0.6	1.08989	1.09167
0.8	1.15441	1.15823
1.0	1.23196	1.23885

TABLE 4

	$\bar{\Omega}_{NL} \times 100$											
	$a/b = 0.5$						$a/b = 1.0$					
A	(0°)		(0°/90°)		(0°/90°/0°)		(0°)		(0°/90°)		(0°/90°/0°)	
	KLT	SDT	KLT	SDT	KLT	SDT	KLT	SDT	KLT	SDT	KLT	SDT
0	1.306	1.227	0.731	0.718	1.286	1.211	1.445	1.360	1.070	1.039	1.445	1.363
0.25	1.327	1.250	0.754	0.741	1.302	1.228	1.467	1.383	1.099	1.069	1.467	1.386
0.5	1.390	1.316	0.818	0.806	1.348	1.277	1.529	1.449	1.181	1.153	1.529	1.452
1.0	1.616	1.553	1.034	1.025	1.520	1.458	1.755	1.686	1.464	1.441	1.757	1.690
1.5	1.935	1.883	1.317	1.310	1.770	1.717	2.079	2.020	1.841	1.824	2.082	2.026
A	(90°/0°/90°)		(0°/90°/90°/0°)		(90°/0°/0°/90°)		(90°/0°/90°)		(0°/90°/90°/0°)		(90°/0°/0°/90°)	
0	0.625	0.613	1.239	1.173	0.715	0.700	1.445	1.323	1.445	1.369	1.445	1.337
0.25	0.645	0.633	1.252	1.187	0.737	0.723	1.467	1.346	1.467	1.392	1.467	1.360
0.5	0.701	0.690	1.291	1.228	0.802	0.789	1.529	1.414	1.529	1.458	1.529	1.427
1.0	0.890	0.882	1.437	1.381	1.020	1.010	1.757	1.658	1.757	1.695	1.757	1.669
1.5	1.138	1.132	1.651	1.603	1.305	1.297	2.082	1.999	2.082	2.030	2.082	2.008
	$a/b = 1.5$						$a/b = 2.0$					
A	(0°)		(0°/90°)		(0°/90°/0°)		(0°)		(0°/90°)		(0°/90°/0°)	
0	1.771	1.668	1.807	1.703	1.831	1.725	2.334	2.187	2.926	2.640	2.501	2.325
0.25	1.794	1.693	1.857	1.756	1.873	1.769	2.365	2.220	3.012	2.736	2.581	2.410
0.5	1.864	1.767	2.003	1.909	1.993	1.895	2.457	2.317	3.262	3.010	2.805	2.649
1.0	2.120	2.035	2.504	2.430	2.414	2.334	2.792	2.670	4.119	3.923	3.563	3.442
1.5	2.488	2.416	3.168	3.111	2.986	2.922	3.275	3.171	5.247	5.095	4.555	4.461
A	(90°/0°/90°)		(0°/90°/90°/0°)		(90°/0°/0°/90°)		(90°/0°/90°)		(0°/90°/90°/0°)		(90°/0°/0°/90°)	
0	2.972	2.457	1.968	1.843	2.883	2.425	5.146	3.798	2.860	2.598	4.956	3.746
0.25	3.009	2.502	2.016	1.894	2.915	2.464	5.209	3.884	2.951	2.698	5.009	3.816
0.5	3.118	2.632	2.152	2.038	3.011	2.576	5.395	4.130	3.209	2.978	5.165	4.019
1.0	3.522	3.100	2.627	2.534	3.367	2.984	6.083	4.995	4.082	3.903	5.748	4.745
1.5	4.108	3.753	3.268	3.194	3.888	3.562	7.082	6.173	5.222	5.083	6.607	5.755

TABLE 5

	$\bar{\Omega}_{NL} \times 100$											
	a/b = 0.5											
	(0º)				(0º/90º)				(0º/90º/0º)			
A	$NH_A=NH_B$		NH_C		$NH_A=NH_B$		NH_C		$NH_A=NH_B$		NH_C	
	KLT	SDT	KLT	SDT	KLT	SDT	KLT	SDT	KLT	SDT	KLT	SDT
0	1.25	1.18	1.25	1.18	0.711	0.697	0.718	0.706	1.211	1.147	1.211	1.147
0.25	1.272	1.203	1.272	1.203	0.729	0.716	0.746	0.735	1.228	1.164	1.228	1.165
0.5	1.338	1.272	1.338	1.272	0.783	0.771	0.823	0.813	1.277	1.216	1.278	1.217
1	1.572	1.516	1.572	1.516	0.968	0.958	1.073	1.065	1.457	1.404	1.458	1.405
1.5	1.898	1.853	1.898	1.853	1.216	1.208	1.392	1.387	1.715	1.67	1.718	1.673
A	(90º/0º/90º)				(0º/90º/90º/0º)				(90º/0º/0º/90º)			
0	0.605	0.595	0.605	0.595	1.155	1.1	1.155	1.1	0.693	0.68	0.693	0.68
0.25	0.625	0.615	0.626	0.616	1.169	1.114	1.169	1.115	0.717	0.704	0.716	0.703
0.5	0.683	0.674	0.684	0.674	1.21	1.158	1.211	1.159	0.783	0.771	0.782	0.77
1	0.876	0.869	0.877	0.87	1.364	1.318	1.365	1.319	1.006	0.997	1.004	0.995
1.5	1.127	1.121	1.128	1.123	1.589	1.549	1.59	1.55	1.294	1.287	1.293	1.285
	a/b = 1.0											
A	(0º)				(0º/90º)				(0º/90º/0º)			
0	1.384	1.308	1.384	1.308	1.044	1.016	1.044	1.015	1.37	1.299	1.37	1.299
0.25	1.406	1.331	1.406	1.331	1.07	1.042	1.077	1.049	1.391	1.322	1.393	1.323
0.5	1.471	1.399	1.471	1.399	1.151	1.125	1.164	1.138	1.456	1.39	1.459	1.393
1	1.705	1.644	1.705	1.644	1.434	1.413	1.456	1.435	1.692	1.636	1.698	1.641
1.5	2.036	1.985	2.036	1.985	1.813	1.797	1.839	1.823	2.026	1.979	2.033	1.986
A	(90º/0º/90º)				(0º/90º/90º/0º)				(90º/0º/0º/90º)			
	KLT	SDT	KLT	SDT	KLT	SDT	KLT	SDT	KLT	SDT	KLT	SDT
0	1.37	1.264	1.37	1.264	1.362	1.297	1.362	1.297	1.362	1.271	1.362	1.271
0.25	1.391	1.287	1.393	1.289	1.385	1.321	1.385	1.321	1.385	1.295	1.385	1.295
0.5	1.456	1.357	1.459	1.36	1.451	1.39	1.451	1.39	1.451	1.365	1.451	1.365
1	1.692	1.608	1.698	1.613	1.689	1.637	1.689	1.637	1.689	1.616	1.689	1.616
1.5	2.026	1.957	2.033	1.963	2.025	1.982	2.025	1.982	2.025	1.965	2.025	1.964
	a/b = 2.0											
A	(0º)				(0º/90º)				(0º/90º/0º)			
0	2.235	2.103	2.235	2.103	2.872	2.622	2.844	2.556	2.423	2.262	2.423	2.262
0.25	2.267	2.138	2.267	2.138	2.972	2.731	2.921	2.642	2.503	2.348	2.505	2.35
0.5	2.513	2.396	2.513	2.396	3.708	3.519	3.467	3.238	3.079	2.954	3.083	2.958
1	2.942	2.844	2.942	2.844	4.866	4.723	4.358	4.179	3.989	3.893	3.994	3.899
1.5	3.205	3.114	3.205	3.114	5.524	5.399	4.876	4.718	4.509	4.425	4.515	4.431
A	(90º/0º/90º)				(0º/90º/90º/0º)				(90º/0º/0º/90º)			
	KLT	SDT	KLT	SDT	KLT	SDT	KLT	SDT	KLT	SDT	KLT	SDT
0	4.846	3.656	4.846	3.656	2.773	2.529	2.773	2.529	4.62	3.576	4.62	3.576
0.25	4.912	3.743	4.915	3.746	2.868	2.633	2.866	2.631	4.676	3.649	4.677	3.649
0.5	5.419	4.388	5.426	4.395	3.532	3.344	3.528	3.34	5.109	4.189	5.112	4.191
1	6.314	5.455	6.323	5.464	4.579	4.435	4.574	4.43	5.88	5.102	5.884	5.104
1.5	6.862	6.081	6.872	6.091	5.178	5.051	5.172	5.045	6.356	5.644	6.361	5.647

TABLE 6

	$\bar{\Omega}_{NL} \times 100$																	
	a / b = 0.5																	
	(0º)						(0º/90º)						(0º/90º/0º)					
A	NH_A		NH_B		NH_C		NH_A		NH_B		NH_C		NH_A		NH_B		NH_C	
	KLT	SDT	KLT	SDT	KLT	SDT	KLT	SDT	KLT	SDT	KLT	SDT	KLT	SDT	KLT	SDT	KLT	SDT
0	1.345	1.256	1.4	1.308	1.204	1.138	0.748	0.733	0.778	0.763	0.679	0.668	1.327	1.243	1.382	1.293	1.183	1.121
0.25	1.366	1.279	1.422	1.331	1.225	1.161	0.77	0.756	0.802	0.787	0.702	0.691	1.343	1.26	1.398	1.311	1.198	1.138
0.5	1.427	1.344	1.485	1.398	1.287	1.226	0.833	0.82	0.867	0.854	0.765	0.755	1.39	1.309	1.446	1.362	1.243	1.185
1	1.648	1.577	1.716	1.641	1.51	1.459	1.046	1.036	1.089	1.078	0.975	0.968	1.561	1.49	1.625	1.551	1.408	1.357
1.5	1.962	1.903	2.043	1.98	1.822	1.78	1.326	1.318	1.381	1.372	1.249	1.243	1.811	1.75	1.885	1.822	1.647	1.603
A	(90º/0º/90º)						(0º/90º/90º/0º)						(90º/0º/0º/90º)					
	KLT	SDT	KLT	SDT	KLT	SDT	KLT	SDT	KLT	SDT	KLT	SDT	KLT	SDT	KLT	SDT	KLT	SDT
0	0.639	0.625	0.665	0.651	0.582	0.572	1.283	1.208	1.335	1.257	1.133	1.08	0.724	0.708	0.754	0.737	0.673	0.66
0.25	0.658	0.644	0.685	0.671	0.602	0.593	1.296	1.222	1.349	1.272	1.146	1.094	0.746	0.73	0.776	0.76	0.696	0.684
0.5	0.71	0.698	0.739	0.727	0.66	0.651	1.336	1.264	1.39	1.315	1.183	1.133	0.807	0.792	0.84	0.825	0.762	0.751
1	0.891	0.881	0.927	0.917	0.852	0.845	1.483	1.418	1.543	1.476	1.322	1.276	1.016	1.004	1.057	1.045	0.981	0.973
1.5	1.129	1.121	1.175	1.167	1.1	1.095	1.7	1.644	1.769	1.711	1.524	1.485	1.291	1.282	1.344	1.334	1.265	1.258
	a / b = 1.0																	
A	(0º)						(0º/90º)						(0º/90º/0º)					
	KLT	SDT	KLT	SDT	KLT	SDT	KLT	SDT	KLT	SDT	KLT	SDT	KLT	SDT	KLT	SDT	KLT	SDT
0	1.489	1.393	1.55	1.45	1.333	1.262	1.095	1.061	1.14	1.104	0.993	0.967	1.489	1.397	1.55	1.454	1.333	1.265
0.25	1.51	1.415	1.572	1.473	1.354	1.284	1.123	1.09	1.169	1.134	1.022	0.996	1.51	1.419	1.572	1.477	1.354	1.287
0.5	1.57	1.48	1.634	1.54	1.415	1.349	1.204	1.173	1.253	1.221	1.102	1.079	1.571	1.483	1.635	1.544	1.416	1.352
1	1.792	1.713	1.865	1.783	1.639	1.582	1.482	1.457	1.543	1.517	1.379	1.36	1.793	1.717	1.866	1.787	1.64	1.586
1.5	2.109	2.043	2.196	2.126	1.955	1.907	1.856	1.836	1.932	1.911	1.745	1.73	2.112	2.048	2.199	2.132	1.958	1.913
A h	(90º/0º/90º)						(0º/90º/90º/0º)						(90º/0º/0º/90º)					
	KLT	SDT	KLT	SDT	KLT	SDT	KLT	SDT	KLT	SDT	KLT	SDT	KLT	SDT	KLT	SDT	KLT	SDT
0	1.489	1.351	1.55	1.406	1.333	1.231	1.489	1.403	1.55	1.46	1.333	1.27	1.489	1.366	1.55	1.421	1.333	1.244
0.25	1.51	1.374	1.572	1.43	1.354	1.254	1.51	1.425	1.572	1.483	1.354	1.292	1.51	1.388	1.572	1.445	1.354	1.267
0.5	1.571	1.44	1.635	1.499	1.416	1.321	1.571	1.489	1.635	1.55	1.416	1.357	1.571	1.454	1.635	1.513	1.416	1.333
1	1.793	1.68	1.866	1.749	1.64	1.559	1.793	1.722	1.867	1.792	1.64	1.59	1.793	1.692	1.867	1.761	1.64	1.569
1.5	2.112	2.017	2.199	2.1	1.958	1.89	2.113	2.053	2.199	2.136	1.958	1.916	2.113	2.027	2.199	2.11	1.958	1.899
	a / b = 2																	
A	(0º)						(0º/90º)						(0º/90º/0º)					
	KLT	SDT	KLT	SDT	KLT	SDT	KLT	SDT	KLT	SDT	KLT	SDT	KLT	SDT	KLT	SDT	KLT	SDT
0	2.405	2.239	2.503	2.33	2.152	2.03	2.992	2.681	3.115	2.79	2.719	2.474	2.558	2.363	2.662	2.46	2.329	2.18
0.25	2.435	2.271	2.535	2.364	2.183	2.063	3.076	2.775	3.202	2.888	2.803	2.568	2.632	2.443	2.74	2.543	2.411	2.267
0.5	2.524	2.366	2.627	2.463	2.273	2.158	3.322	3.045	3.457	3.17	3.05	2.835	2.843	2.669	2.959	2.778	2.642	2.511
1	2.851	2.712	2.967	2.823	2.604	2.504	4.166	3.95	4.336	4.111	3.886	3.72	3.564	3.427	3.71	3.567	3.411	3.31
1.5	3.326	3.208	3.461	3.338	3.077	2.993	5.284	5.116	5.5	5.325	4.978	4.851	4.517	4.41	4.702	4.59	4.403	4.326
A	(90º/0º/90º)						(0º/90º/90º/0º)						(90º/0º/0º/90º)					
	KLT	SDT	KLT	SDT	KLT	SDT	KLT	SDT	KLT	SDT	KLT	SDT	KLT	SDT	KLT	SDT	KLT	SDT
0	5.311	3.828	5.528	3.984	4.733	3.587	2.898	2.616	3.016	2.723	2.694	2.463	5.134	3.787	5.343	3.941	4.535	3.522
0.25	5.374	3.915	5.594	4.075	4.794	3.668	2.984	2.712	3.106	2.822	2.787	2.565	5.187	3.859	5.399	4.017	4.586	3.587
0.5	5.56	4.165	5.787	4.335	4.973	3.899	3.23	2.98	3.362	3.101	3.049	2.847	5.344	4.068	5.563	4.234	4.735	3.775
1	6.246	5.045	6.501	5.251	5.634	4.713	4.065	3.87	4.231	4.028	3.926	3.772	5.932	4.814	6.174	5.011	5.288	4.45
1.5	7.246	6.241	7.542	6.496	6.59	5.822	5.166	5.014	5.377	5.218	5.061	4.942	6.8	5.85	7.077	6.089	6.099	5.389